Naval Research Laboratory
Washington, DC 20375-5000

NRL Report 9316

Theory and Application of the Wavelet Transform to Signal Processing

D. M. DRUMHELLER

Acoustic Systems Branch
Acoustics Division

July 31, 1991

DISCLAIMER NOTICE

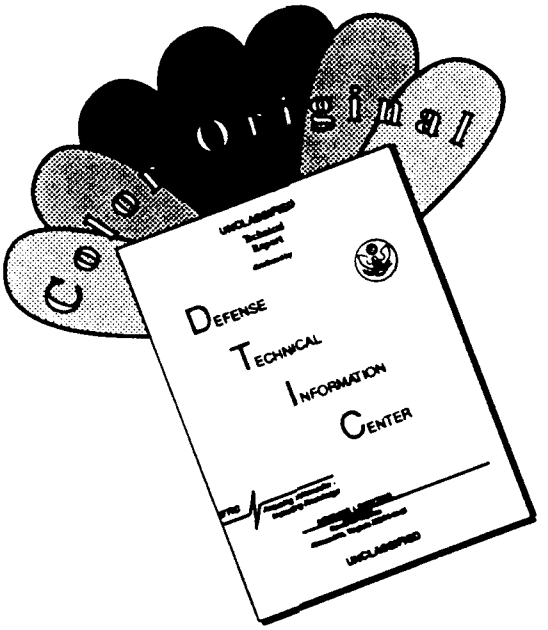

THIS DOCUMENT IS BEST QUALITY AVAILABLE. THE COPY FURNISHED TO DTIC CONTAINED A SIGNIFICANT NUMBER OF COLOR PAGES WHICH DO NOT REPRODUCE LEGIBLY ON BLACK AND WHITE MICROFICHE.

REPORT DOCUMENTATION PAGE

Form Approved
OMB No 0704-0188

1. AGENCY USE ONLY *(Leave blank)*	2. REPORT DATE	3. REPORT TYPE AND DATES COVERED
	July 31, 1991	NRL Report May 1990 to October 1990

4. TITLE AND SUBTITLE

Theory and Application of the Wavelet Transform to Signal Processing

5. FUNDING NUMBERS

PE — 62435N
PR — RJ35B01
WU — DN480-045

6. AUTHOR(S)

Drumheller, David M.

7. PERFORMING ORGANIZATION NAME(S) AND ADDRESS(ES)

Naval Research Laboratory
Washington, DC 20375-5000

8. PERFORMING ORGANIZATION REPORT NUMBER

NRL Report 9316

9. SPONSORING/MONITORING AGENCY NAME(S) AND ADDRESS(ES)

Office of Naval Technology
Arlington, VA 22217

10. SPONSORING/MONITORING AGENCY REPORT NUMBER

90-165

11. SUPPLEMENTARY NOTES

12a. DISTRIBUTION/AVAILABILITY STATEMENT

Approved for public release; distribution is unlimited.

12b. DISTRIBUTION CODE

13. ABSTRACT *(Maximum 200 words)*

Recently, a new representation of square summable functions has been found that displays some sense of locality in time. Its continuous version is called the wavelet transform, and discrete version is called the wavelet expansion. This report presents several theoretical and practical aspects of these new representations in the context of signal theory and a signal processing. On the theoretical level, some new results are proved regarding the properties of wavelets. The work of others has also been extended. Two practical applications of the wavelet expansion are also presented. The first is the equivalent to passband filtering of analog signals, and the second is the derivation of an iterative restoration algorithm used to estimate the impulse response of a linear system.

14. SUBJECT TERMS			15. NUMBER OF PAGES
	Wavelet	Orthogonal expansion	50
	Linear systems	Stochastic signals	16. PRICE CODE
	Filtering	Deconvolution	

17. SECURITY CLASSIFICATION OF REPORT	18. SECURITY CLASSIFICATION OF THIS PAGE	19. SECURITY CLASSIFICATION OF ABSTRACT	20. LIMITATION OF ABSTRACT
UNCLASSIFIED	UNCLASSIFIED	UNCLASSIFIED	UL

NSN 7540-01-280-5500

Standard Form 298 (Rev 2-89)
Prescribed by ANSI Std 239-18
298-102

CONTENTS

1. INTRODUCTION 1

2. THE WAVELET TRANSFORM 2

3. PROPERTIES OF THE WAVELET TRANSFORM 5

4. LINEAR SYSTEMS AND THE WAVELET TRANSFORM 8

5. THE WAVELET EXPANSION AND DAUBECHIES WAVELETS 13

6. PROPERTIES OF DAUBECHIES WAVELETS 17

7. APPLICATION: WAVELET PASSBAND FILTERING 25

8. APPLICATION: A DECONVOLUTION ALGORITHM 31

9. SUMMARY 39

10. REFERENCES 40

APPENDIX A — Fourier Series Coefficients for Daubechies Wavelets 43

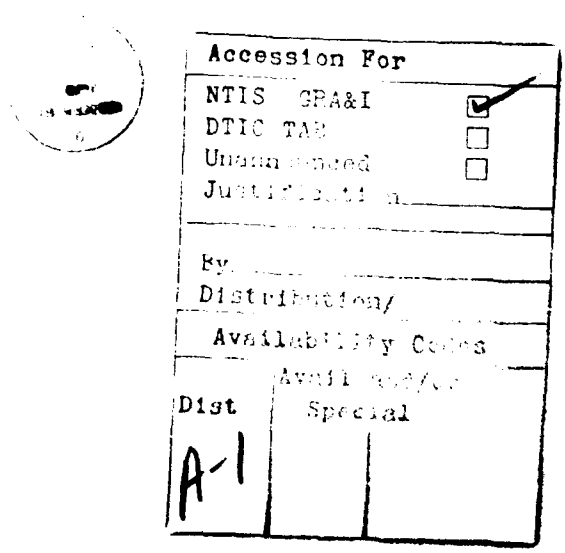

THEORY AND APPLICATION OF THE WAVELET TRANSFORM TO SIGNAL PROCESSING

1. INTRODUCTION

Most scientists and engineers are familar with the Fourier representation of a function. In most cases of practical interest, it is well known that a piecewise continuous periodic function $g_T(t)$ can be equated almost everywhere with a weighted countably infinite sum of exponential functions, i.e.,

$$g_T(t) \stackrel{a.e.}{=} \sum_{n=-\infty}^{\infty} g_n e^{j2\pi nt/T}, \tag{1}$$

where g_n is the nth Fourier coefficient, and is given by

$$g_n = \frac{1}{T}\int_0^T g_T(t)e^{-j2\pi nt/T}dt. \tag{2}$$

This is the classic Fourier series. The Fourier representation for a piecewise continuous nonperiodic function $g(t)$ has the integral formulation

$$g(t) \stackrel{a.e.}{=} \int_{-\infty}^{\infty} G(f)e^{j2\pi ft}df, \tag{3}$$

where $G(f)$ is the Fourier transform of $g(t)$, and is given by

$$G(f) = \int_{-\infty}^{\infty} g(t)e^{-j2\pi ft}dt. \tag{4}$$

The development of Fourier theory constitutes a significant portion of classical mathematical analysis. It has also been a valuable tool in physics and engineering by contributing to the solution of problems in linear system theory, thermodynamics, and quantum physics, to name a few.

Despite their wide use, some problems arise in the interpretation of the classic Fourier representations. For example, if $g(t)$ is a function that is nonzero only in an interval (it has compact support), then the Fourier transform implies that this time-limited function is a summation of complex exponential functions, each having support over the entire real line. Furthermore, one cannot associate features of the time function $g(t)$ with any specific value, or range of values, of f of the transform $G(f)$. In other words, the transform exhibits no locality of time; a transient feature in $g(t)$ contributes to $G(f)$ at all values of f.

Manuscript approved March 4, 1991.

In light of these observations, researchers have sought alternatives to the Fourier representations that display some sense of locality in time. It was recently discovered that certain functions, those whose amplitude is significant over a finite interval, can serve as a transform kernel for square summable functions, provided they obey a regularity condition [1-5]. These functions are defined as a time-dilated and time-shifted version of a specified function $\psi(t)$ called a *wavelet*. Thus, the transform kernel is $\psi(s(t-\tau))$, where $s \in [0, \infty)$, and $\tau \in (-\infty, \infty)$. If we integrate the function $g(t)$ with respect to this kernel, the result is the *wavelet transform* $\phi_g(s, \tau)$, which is analogous to the Fourier transform since it has an integral representation for both the forward and inverse transform. There is also a version of it analogous to the Fourier series in that it represents a function as a countable sum of wavelets.

Many uses for the wavelet transform have been proposed [1]. Among them are the identification and localization of transients in time series and the compact coding of images if the concept of a wavelet is extended to two dimensions. In this report we are concerned with the application of the wavelet transform in signal theory and signal processing. The first part of the report presents several theorems, some of which are results that have either been left unproven in other references or have only been alluded to by other authors. Others are new, and present a deliberate attempt to reformulate some standard signal theory in the context of the wavelet transform. The last part of the report presents the application of the wavelet transform to two common signal processing problems: filtering and deconvolution.

Throughout this report we maintain the following notational conventions: time signals are represented by lower case italic as in $g(t)$, and their associated Fourier transforms are always written with the same letter but in upper case italic as in $G(f)$. Vectors are written in bold lower case italic as in $\boldsymbol{x}$, and matrices are written in bold upper case italic as in $\boldsymbol{A}$. Finally, it is assumed that the reader has some familiarity with real analysis.

2. THE WAVELET TRANSFORM

As the Fourier transform does, the wavelet transform also provides a representation of the elements in the set of all square summable functions. This is the space $L^2(R)$, where R denotes the real line. The wavelet transform of the function $g(t)$ is given by

$$\mathcal{W}\left\{g(t)\right\} = \phi_g(s,\tau) = \sqrt{s}\int_{-\infty}^{\infty} g(t)\psi^*(s(t-\tau))dt, \tag{5}$$

where $\psi(t)$ is referred to as the *analyzing wavelet*, s is the *dilation variable*, and τ is the *delay variable*. This defines a mapping from the one-dimensional (1-D) time domain, to the two-dimensional (2-D) dilation/delay space defined by the (s,τ) plane. The factor $\sqrt{s}$ appears because

$$s\int_{-\infty}^{\infty} |\psi(s(t-\tau))|^2 dt = \int_{-\infty}^{\infty} |\psi(t)|^2 dt, \tag{6}$$

thereby acting as a normalization factor. This implies the relative amplitudes, or powers (square magnitude), of the wavelet transform at two different points in the (s,τ) plane can be compared meaningfully.

Note in the mathematical literature that the time-dilated and time-shifted version of the analyzing wavelet is defined as

$$\frac{1}{\sqrt{a}}\psi\left(\frac{t-\tau}{a}\right), \tag{7}$$

where $a = 1/s$, and $a \in [0,\infty)$. We choose the definition by using s rather than a since it is often interpreted as the time-dilation due to the Doppler effect caused by a moving point reflector. That is, if a transmitter is stationary and a reflector is moving with a positive radial velocity of v, then

$$s = \frac{1-v/c}{1+v/c} \simeq 1 - \frac{2v}{c}, \tag{8}$$

where c is the propagation speed. Thus, if we transmit the signal $g(t)$, then we receive $\sqrt{s}g(st)$. Adopting the convention of modeling time-dilation by the variable s will make the results presented in this report immediately applicable to those working in the field of wideband echo-location systems.

Given the definition of a forward transform in Eq. (5), we naturally seek a formula for transforming from the (s,τ) plane back to the time domain. If the wavelet's Fourier transform $\Psi(f)$ meets a regularity condition, namely

$$C_\psi = \int_0^\infty \frac{|\Psi(f)|^2}{f} df < \infty, \tag{9}$$

and $|\Psi(f)| = |\Psi(-f)|$, then an inversion formula for the wavelet transform exists, and $g(t)$ can be recovered from $\phi_g(s,\tau)$ through the formula

$$g(t) \overset{\text{a.e.}}{=} \frac{1}{C_\psi}\int_{s=0}^\infty \int_{\tau=-\infty}^\infty \sqrt{s}\,\phi_g(s,\tau)\psi(s(t-\tau))d\tau ds. \tag{10}$$

For completeness, a proof of this result is given below since most published versions of it can only be found in obscure references.

Proof of the Inversion Formula - We begin by substituting Eq. (5) into Eq. (10) to get

$$I = \frac{1}{C_\psi}\int_{s=0}^\infty \int_{\tau=-\infty}^\infty s\left[\int_{-\infty}^\infty g(y)\psi^*(s(y-\tau))dy\right]\psi(s(t-\tau))d\tau ds. \tag{11}$$

However, it can be shown that the Fourier transform of $\psi(s(t-\tau))$ is given by

$$\mathcal{F}\left\{\psi(s(t-\tau))\right\} = \int_{-\infty}^\infty \psi(s(t-\tau))e^{-j2\pi ft}dt = \frac{\Psi(f/s)}{s}e^{-j2\pi f\tau}. \tag{12}$$

Therefore, by invoking Parseval's Theorem, using Eq. (12), and defining $G(f)$ to be the Fourier transform of $g(t)$ ($G(f)$ exits since $g(t) \in L^2(R)$), one finds that

$$\begin{aligned} I &= \frac{1}{C_\psi}\int_{s=0}^{\infty}\int_{\tau=-\infty}^{\infty} s\left[\int_{-\infty}^{\infty} G(f)\frac{\Psi^*(f/s)}{s}e^{\jmath 2\pi f\tau}df\right]\left[\int_{-\infty}^{\infty}\frac{\Psi(\xi/s)}{s}e^{\jmath 2\pi\xi(t-\tau))}d\xi\right]d\tau ds \\ &= \frac{1}{C_\psi}\int_{s=0}^{\infty}\int_{f=-\infty}^{\infty} s^{-1}G(f)\Psi^*(f/s)\left[\int_{-\infty}^{\infty}\int_{-\infty}^{\infty}\Psi(\xi/s)e^{\jmath 2\pi(f\tau+\xi(t-\tau))}d\tau d\xi\right]df ds. \quad (13) \end{aligned}$$

The bracketed factor in the integrand of the last line of Eq. (13) can be reduced as follows:

$$\begin{aligned} \int_{-\infty}^{\infty}\int_{-\infty}^{\infty}\Psi(\xi/s)e^{\jmath 2\pi(f\tau+\xi(t-\tau))}d\tau d\xi &= \int_{-\infty}^{\infty}\left[\int_{-\infty}^{\infty}\Psi(\xi/s)e^{\jmath 2\pi\xi(t-\tau)}d\xi\right]e^{2\jmath\pi f\tau}d\tau \\ &= \int_{-\infty}^{\infty} s\psi(s(t-\tau))e^{\jmath 2\pi f\tau}d\tau \\ &= \int_{-\infty}^{\infty}\psi(z)e^{\jmath 2\pi(f/s)z}dz\ e^{\jmath 2\pi ft} \\ &= \Psi(f/s)e^{\jmath 2\pi ft}. \quad (14) \end{aligned}$$

Thus, substituting Eq. (14) into Eq. (13) yields

$$\begin{aligned} I &= \frac{1}{C_\psi}\int_{s=0}^{\infty}\int_{f=-\infty}^{\infty} s^{-1}G(f)|\Psi(f/s)|^2e^{\jmath 2\pi ft}df ds \\ &= \frac{1}{C_\psi}\int_{-\infty}^{\infty} G(f)\left[\int_0^{\infty} s^{-1}|\Psi(f/s)|^2ds\right]e^{\jmath 2\pi ft}df. \quad (15) \end{aligned}$$

Concerning the bracketed factor in the integrand of Eq. (15), if $f \neq 0$, then the change of variable $\eta = s/f$ yields

$$\int_0^{\infty} s^{-1}|\Psi(f/s)|^2ds = \int_0^{\infty}\frac{|\Psi(\eta)|^2}{\eta}d\eta = C_\psi. \quad (16)$$

Note that this is true regardless of the sign of f since $|\Psi(f)| = |\Psi(-f)|$ by hypothesis. We now consider the value of the bracketed factor as $f \to 0$. In this case

$$\begin{aligned} \lim_{f\to 0}\int_0^{\infty} s^{-1}|\Psi(f/s)|^2ds &= \lim_{f\to 0}\left[\lim_{a\to 0^+}\int_a^{1/a} s^{-1}|\Psi(f/s)|^2ds\right] \\ &= \lim_{f\to 0}\left[\lim_{a\to 0^+}\int_{fa}^{f/a} z^{-1}|\Psi(z)|^2dz\right] \\ &= \lim_{f\to 0} C_\psi \\ &= C_\psi \quad (17) \end{aligned}$$

This result can also be deduced by noting that for any $|f| > 0$, however small, Eq. (16) always holds. Hence, the value of the limit of the integral in Eq. (16) is C_ψ. Regardless of its value at $f = 0$, we at least know that

$$\int_0^{\infty}|\Psi(f/s)|^2ds = C_\psi \text{ for almost all } f. \quad (18)$$

In light of Eq. (18), Eq. (15) reduces to

$$I = \int_{-\infty}^{\infty} G(f) e^{j2\pi ft} df \overset{a.e.}{=} g(t), \tag{19}$$

which proves the inversion formula in Eq. (10). This completes the proof.

3. PROPERTIES OF THE WAVELET TRANSFORM

We now state and prove three properties of the wavelet transform. The first property concerns the wavelet transform of a time-dilated and time-shifted signal.

Theorem 1: Let $\phi_g(s,\tau)$ be the wavelet transform of the function $g(t)$. Then for $s_0 > 0$,

$$\mathcal{W}\left\{\sqrt{s_0} g(s_0(t-\tau_0))\right\} = \phi_g\left(\frac{s}{s_0}, s_0(\tau-\tau_0)\right). \tag{20}$$

Proof of Theorem 1: Equation (20) follows directly from the definition of the wavelet transform by substituting $\sqrt{s_0} g(s_0(t-\tau))$ for $g(t)$ in the integrand of Eq. (5), and by invoking the change of variable $y = s_0(t-\tau_0)$. This completes the proof.

The theorem above shows how distortion in the time domain affects the wavelet transform. For example, if $s_0 > 1$, we see that the support of the wavelet transform in the (s,τ) becomes wider in s and narrower in τ. Delaying a function in time merely delays its wavelet transform along the τ axis.

As in the case of the Fourier transform, one is often concerned about how rapidly the transform $G(f)$ decays as $|f| \to 0$. This 'decay rate' is related to the continuity of $g(t)$. The following theorem describes the decay rate of the wavelet transform $\phi_g(s,\tau)$ at points of continuity, and at points of a jump discontinuity for the function $g(t)$, providing $g(t)$ is of bounded variation.

Theorem 2: Let $g(t) \in L^2(R)$ and $\psi(t) \in L^1(R) \bigcap L^2(R)$. Suppose $g(t)$ is of bounded variation in a neighborhood of t_0, then the wavelet transform of $g(t)$ with respect to the wavelet $\psi(t)$ has the property

$$(i)\ \ \phi_g(s,t_0) \to 0 \text{ as } s \to \infty.$$

Furthermore, if for all $\delta > 0$,

$$s \int_{|z|>s\delta} |\psi(z)|^2 dz \to 0 \text{ as } s \to \infty, \tag{21}$$

then if $g(t)$ has a finite jump discontinuity at t_0, then

$$(ii)\ \ \sqrt{s}\phi_g(s,t_0) \to g(t_0^-)\psi_-^* + g(t_0^+)\psi_+^* \text{ as } s \to \infty,$$

where

$$\begin{aligned} \psi_+ &= \int_0^\infty \psi(t)dt, \\ \psi_- &= \int_{-\infty}^0 \psi(t)dt. \end{aligned} \tag{22}$$

If $g(t)$ is continuous at t_0, then

$$(iii)\ \ \sqrt{s}\phi_g(s,t_0) \to 0 \text{ as } s \to \infty.$$

Proof of Theorem 2: We note that for any $\delta > 0$,

$$\begin{aligned} \phi_g(s,t_0) &= \sqrt{s}\int_{-\infty}^{\infty} g(t)\psi^*(s(t-t_0))dt \\ &= \int_{|t-t_0|>\delta} + \int_{|t-t_0|\le\delta} \sqrt{s}g(t)\psi^*(s(t-t_0))dt \\ &= I_1 + I_2. \end{aligned} \tag{23}$$

Consider I_1 and I_2, one at a time.

We first show that $I_1 \to 0$ as $s \to \infty$. By the Schwartz inequality

$$\begin{aligned} 0 \le |I_1|^2 &\le \|g\|_2^2 \int_{|t-t_0|>\delta} s|\psi(s(t-t_0))|^2 dt \\ &= \|g\|_2^2 \int_{|z|>s\delta} |\psi(z)|^2 dz. \end{aligned} \tag{24}$$

But since $\delta > 0$,

$$\lim_{s\to\infty} \int_{|z|>s\delta} |\psi(z)|^2 dz = \lim_{s\to\infty} \int_{-\infty}^{-s\delta} + \int_{s\delta}^{\infty} |\psi(z)|^2 dz = \int_{-\infty}^{-\infty} + \int_{\infty}^{\infty} |\psi(z)|^2 dz = 0+0 = 0. \tag{25}$$

(This could also have been proved by using the density of the step functions in $L^2(R)$.) Thus, by applying the squeeze theorem for limits to Eq. (24) one finds that

$$\lim_{s\to\infty} |I_1|^2 = 0 \Rightarrow \lim_{s\to\infty} I_1 = 0. \tag{26}$$

Furthermore, if Eq. (21) is true, then by a similar development

$$0 \le |\sqrt{s}I_1|^2 \le \|g\|_2^2 \int_{|z|>s\delta} s|\psi(z)|^2 dz \to 0 \text{ as } s \to \infty, \tag{27}$$

which proves

$$\sqrt{s}I_1 \to 0 \text{ as } s \to \infty. \tag{28}$$

Now consider I_2. It is sufficient to consider the case where $g(t)$ and $\psi(t)$ are real valued. Because $g(t)$ is of bounded variation in a neighborhood of t_0, say $[t_0-\delta, t_0+\delta]$, we

know $g(t)$ is the difference of two increasing function (that are also of bounded variation). Therefore, it is also sufficient to consider the case of $g(t)$ increasing, and with a finite jump discontinuity at t_0.

Using the second mean value theorem for integrals, we note that for some $\eta \in (t_0, t_0+\delta]$,

$$\begin{aligned}
\int_{t_0}^{t_0+\delta} g(t)s\psi(s(t-t_0))dt &= \int_{t_0}^{\eta} + \int_{\eta}^{t_0+\delta} g(t)s\psi(s(t-t_0))dt \\
&= g(t_0^+)\int_{t_0}^{\eta} s\psi(s(t-t_0))dt \\
&\qquad + g(t_0+\delta)\int_{\eta}^{t_0+\delta} s\psi(s(t-t_0))dt \\
&= g(t_0^+)\int_0^{s(\eta-t_0)} \psi(z)dz + g(t_0+\delta)\int_{s(\eta-t_0)}^{s\delta} \psi(z)dz \\
&\to g(t_0^+)\psi_+ + g(t_0+\delta)\int_{\infty}^{\infty} \psi(z)dz \\
&\qquad = g(t_0^+)\psi_+ \text{ as } s \to \infty, \qquad (29)
\end{aligned}$$

where we have used the definitions of ψ_- and ψ_+ given in Eq. (22). Similarly,

$$\int_{t_0-\delta}^{t_0} g(t)s\psi(s(t-t_0))dt \to g(t_0^-)\psi_- \text{ as } s \to \infty. \qquad (30)$$

Together Eqs. (29) and (30) show that

$$\sqrt{s}I_2 \to g(t_0^-)\psi_- + g(t_0^+)\psi_+ < \infty \text{ as } s \to \infty. \qquad (31)$$

This, in turn, implies that

$$I_2 \to 0 \text{ as } s \to \infty. \qquad (32)$$

For if $I_2 \to K \neq 0$ as $s \to \infty$, then $\sqrt{s}I_2 \to \infty$ as $s \to \infty$, which contradicts Eq. (31).

Equations (26) and (32) prove property (i), and Eqs. (28) and (31) prove property (ii). If $g(t)$ is continuous at t_0, then $g(t_0^-) = g(t_0^+)$, and property (iii) follows immediately. This completes the proof.

Properties (ii) and (iii) imply that at $t = t_0$ the wavelet transform falls off to 0 less rapidly along the s axis if $g(t)$ has a jump discontinuity at t_0. In other words, any discontinuous jump of the function $g(t)$ at $t = t_0$ implies the value of $\phi_g(s, t_0)$ is significant for large values of s. In a practical sense, this means that the wavelet transform can be used for transient detection, since any abrupt change or short term feature of the function should cause $\phi_g(s, t_0)$ to be significant for large values of s. Also, because of the assumed regularity of the wavelet, we know $\Psi(0) = 0$, hence

$$0 = \Psi(0) = \int_{-\infty}^{\infty} \psi(t)dt = \psi_- + \psi_+ \Rightarrow \psi_+ = -\psi_-. \qquad (33)$$

Furthermore, the condition $\psi \in L^1(R)$ implies ψ_+ and ψ_- are finite since

$$|\psi_+|, |\psi_-| \leq \int_{-\infty}^{\infty} |\psi(t)| dt = \|\psi\|_1 < \infty. \tag{34}$$

Finally, almost any function encountered in practice modeling a physical phenomenon will be a well behaved, bounded, piece-wise continuous function. Thus, requiring $g(t)$ to be of bounded variation is not overly restrictive.

Theorem 3: Suppose $g(t)$ and the wavelet $\psi(t)$ are members of $L^2(R)$, then

$$|\phi_g(s,\tau)|^2 \leq \|g\|_2^2 \, \|\psi\|_2^2. \tag{35}$$

Proof of Theorem 3: Equation (35) follows directly from the application of the Schwartz inequality to Eq. (5):

$$\begin{aligned} |\psi_g(s,\tau)|^2 &= \left| \sqrt{s} \int_{-\infty}^{\infty} g(t) \psi^*(s(t-\tau)) dt \right|^2 \\ &\leq \left[\int_{-\infty}^{\infty} |g(t)|^2 dt \right] \left[s \int_{-\infty}^{\infty} |\psi(s(t-\tau)|^2 dt \right] \\ &= \left[\int_{-\infty}^{\infty} |g(t)|^2 dt \right] \left[\int_{-\infty}^{\infty} |\psi(z)|^2 dz \right] \\ &= \|g\|_2^2 \, \|\psi\|_2^2. \end{aligned} \tag{36}$$

4. LINEAR SYSTEMS AND THE WAVELET TRANSFORM

In this section we state and prove three results of the wavelet transform as applied to linear system theory.

Theorem 4: Let $x(t)$ be the deterministic input to a linear system whose known impulse response is $g(t)$, and whose output is $y(t) = x(t) * g(t)$, where $*$ denotes the convolution operator. Furthermore, let the wavelet transforms of $x(t)$, $g(t)$, and $y(t)$ be given by

$$\begin{aligned} \mathcal{W}\left\{x(t)\right\} &= \phi_x(s,\tau) = \sqrt{s} \int_{-\infty}^{\infty} x(t) \psi^*(s(t-\tau)) dt, \\ \mathcal{W}\left\{y(t)\right\} &= \phi_g(s,\tau) = \sqrt{s} \int_{-\infty}^{\infty} g(t) \psi^*(s(t-\tau)) dt, \\ \mathcal{W}\left\{y(t)\right\} &= \phi_y(s,\tau) = \sqrt{s} \int_{-\infty}^{\infty} y(t) \psi^*(s(t-\tau)) dt. \end{aligned} \tag{37}$$

Then the wavelet transform of the output $y(t)$ is related to the wavelet transforms of $x(t)$ and $g(t)$ through the equation

$$\phi_y(s,\tau) = \int_{-\infty}^{\infty} x(z) \phi_g(s, z-\tau) dz = \int_{-\infty}^{\infty} g(z) \phi_x(s, z-\tau) dz. \tag{38}$$

Proof Theorem 4: First, it is well known from linear system theory that

$$y(t) = \int_{-\infty}^{\infty} x(z)g(t-z)dz = x(t) * g(t). \tag{39}$$

Substituting Eq. (39) into the definition of the wavelet transform of $y(t)$, and invoking a change of variable yields

$$\begin{aligned}
\mathcal{W}\left\{y(t)\right\} &= \phi_y(s,\tau) \\
&= \sqrt{s}\int_{-\infty}^{\infty} y(t)\psi^*(s(t-\tau))dt \\
&= \sqrt{s}\int_{-\infty}^{\infty}\int_{-\infty}^{\infty} x(z)g(t-z)\psi^*(s(t-\tau))dtdz \\
&= \int_{-\infty}^{\infty} x(z)\left[\sqrt{s}\int_{-\infty}^{\infty} g(t-z)\psi^*(s(t-\tau))dt\right]dz \\
&= \int_{-\infty}^{\infty} x(z)\left[\sqrt{s}\int_{-\infty}^{\infty} g(t)\psi^*(s(t-(\tau-z))dt\right]dz \\
&= \int_{-\infty}^{\infty} x(z)\phi_g(s,\tau-z)dz,
\end{aligned} \tag{40}$$

which proves the first integral in Eq. (38). The second integral in Eq. (38) is derived similarly, but starts with the alternate form of the convolution integral

$$y(t) = \int_{-\infty}^{\infty} g(z)x(t-z)dz. \tag{41}$$

This completes the proof.

It is well known from the theory of stochastic processes that the autocorrelation function of a stationary process $x(t)$ is related to its power spectral density $S_{xx}(f)$ through the Fourier transform relation

$$E\{x(t)x^*(t-z)\} = R_{xx}(z) = \int_{-\infty}^{\infty} S_{xx}(f)e^{j2\pi fz}df. \tag{42}$$

This is known as the Weiner-Khinchine Theorem [6]. Furthermore, if $x(t)$ is passed through a linear time-invariant filter whose impulse response is $g(t)$, then the power spectral density of the output $y(t)$ [6] is given by:

$$S_{yy}(f) = \left|\mathcal{F}\left\{g(t)\right\}\right|^2 S_{xx}(f). \tag{43}$$

The following theorem gives similar relationships for the wavelet transform.

Theorem 5: Let $x(t)$ be a wide-sense stationary stochastic process whose autocorrelation function is defined by

$$R_{xx}(z) = E\{x(t)x^*(t \quad z)\}. \tag{44}$$

Then the wavelet transform of the autocorrelation function with respect to the wavelet $\psi(t)$ is given by

$$\mathcal{W}\left\{R_{xx}(z)\right\} = \phi_{xx}(s,\tau) = \sqrt{s}\int_{-\infty}^{\infty} R_{xx}(z)\psi^*(s(z-\tau))dz, \tag{45}$$

and the Fourier transform of $\phi_{xx}(s,\tau)$ with respect to τ is

$$\mathcal{F}\left\{\phi_{xx}(s,\tau)\right\} = \Phi_{xx}(s,f) = \frac{\Psi^*(f/s)}{\sqrt{s}} S_{xx}(f), \tag{46}$$

where $\Psi(f)$ is the Fourier transform of the wavelet $\psi(t)$, and $S_{xx}(f)$ is the power spectral density of $x(t)$. Furthermore, let $x(t)$ drive a linear time-invariant system whose impulse response is $g(t)$, and whose output is denoted by $y(t)$. Then the Fourier transform of the wavelet transform of the output autocorrelation function $R_{yy}(z)$ is given by

$$\Phi_{yy}(s,f) = |G(f)|^2 \Phi_{xx}(s,f). \tag{47}$$

Proof of Theorem 5 (first method): We take the wavelet transform of the autocorrelation function directly, and use the Fourier transform property (a transformation with respect to the variable t)

$$\mathcal{F}\left\{\sqrt{s}\psi^*(s(t-\tau))\right\} = \frac{\Psi^*(-f/s)e^{-\jmath 2\pi f\tau}}{\sqrt{s}}, \tag{48}$$

where $s \geq 0$. Thus,

$$\begin{aligned}
\mathcal{W}\left\{R_{xx}(z)\right\} &= \sqrt{s}\int_{-\infty}^{\infty} R_{xx}(z)\psi^*(s(t-\tau))dz \\
&= s^{-1/2}\int_{-\infty}^{\infty} R_{xx}(z)\left[\int_{-\infty}^{\infty} \Psi^*(-f/s)e^{\jmath 2\pi f(z-\tau)}df\right]dz \\
&= s^{-1/2}\int_{-\infty}^{\infty} \Psi^*(-f/s)\left[\int_{-\infty}^{\infty} R_{xx}(z)e^{\jmath 2\pi fz}dz\right]e^{-\jmath 2\pi f\tau}df \\
&= s^{-1/2}\int_{-\infty}^{\infty} \Psi^*(-f/s)S_{xx}(-f)e^{-\jmath 2\pi f\tau}df \\
&= s^{-1/2}\int_{-\infty}^{\infty} \Psi^*(f/s)S_{xx}(f)e^{\jmath 2\pi f\tau}df.
\end{aligned} \tag{49}$$

Therefore,

$$\phi_{xx}(s,\tau) = \mathcal{F}^{-1}\left\{\frac{\Psi^*(f/s)}{\sqrt{s}} S_{xx}(f)\right\}. \tag{50}$$

This, in turn, implies that

$$\Phi_{xx}(s,f) = \frac{\Psi^*(f/s)}{\sqrt{s}} S_{xx}(f), \tag{51}$$

which proves Eq. (46).

If we now consider the case of $x(t)$ driving a linear system whose impulse response is $g(t)$, then from Eq. (43) the power spectral density of the output $y(t)$ is

$$S_{yy}(f) = |G(f)|^2 S_{xx}(f). \tag{52}$$

Thus, from Eq. (51) and (52) it follows that

$$\begin{aligned}
\Phi_{yy}(s,f) &= \frac{\Psi^*(f/s)}{\sqrt{s}} S_{yy}(f) \\
&= \frac{\Psi^*(f/s)}{\sqrt{s}} |G(f)|^2 S_{xx}(f) \\
&= |G(f)|^2 \left[\frac{\Psi^*(f/s)}{\sqrt{s}} S_{xx}(f) \right] \\
&= |G(f)|^2 \Phi_{xx}(s,f),
\end{aligned} \tag{53}$$

which proves Eq. (47). This completes the proof.

Proof of Theorem 5 (second method): This approach uses the definition of the autocorrelation as an expectation. Substituting Eq. (44) into Eq. (45), and using the change of variable $w = t - z$ yields

$$\begin{aligned}
\mathcal{W}\left\{R_{xx}(z)\right\} &= \sqrt{s}\int_{-\infty}^{\infty} E\{x(t)x^*(t-z)\}\psi^*(s(z-\tau))dz \\
&= E\left\{x(t)\sqrt{s}\int_{-\infty}^{\infty} x^*(t-z)\psi^*(s(z-\tau))dz\right\} \\
&= E\left\{x(t)\left[\sqrt{s}\int_{-\infty}^{\infty} x(w)\psi(s((t-\tau)-w))dw\right]^*\right\} \\
&= E\{z(t)h^*(t-\tau)\},
\end{aligned} \tag{54}$$

where we interpret $h(t)$ to be the response to the input $x(t)$ of a linear time-invariant system whose impulse response is $\sqrt{s}\psi(st)$. Thus, the last line in Eq. (54) is the cross-correlation function $R_{xh}(\tau)$. The Fourier transform of this correlation function is the cross-power spectral density function, and it is well known that

$$\mathcal{F}\left\{R_{xh}(\tau)\right\} = S_{xh}(f) = \frac{\Psi^*(f/s)}{\sqrt{s}} S_{xx}(f), \tag{55}$$

where we have used the Fourier transform relation

$$\mathcal{F}\left\{\sqrt{s}\psi(st)\right\} = \frac{\Psi(f/s)}{\sqrt{s}}. \tag{56}$$

We note, however, that Eq. (55) is also equal to the Fourier transform with respect to τ of the wavelet transform $\phi_{xx}(s,\tau)$. Thus, we have proved Eq. (46). The proof of Eq. (47) is identical to the approach used in the first method. This completes the proof.

Let $R(s,\tau)$ be a density function that describes the average amount of spread in range delay τ and Doppler variable s a signal undergoes when applied to a dispersive channel. We call $R(s,\tau)$ the channel *scattering function* [7,8]. Furthermore, if the input signal to the channel is $x(t)$, and its wavelet transform is

$$\mathcal{W}\{x(t)\} = \phi_x(s,\tau) = \sqrt{s}\int_{-\infty}^{\infty} x(t)\psi^*(s(t-\tau))dt, \tag{57}$$

then the expected square magnitude of the wavelet transform of the channel output $y(t)$ is given by

$$E\{|\phi_y(s,\tau)|^2\} = \int_{z=-\infty}^{\infty}\int_{w=0}^{\infty} R(w,z)A_{x\psi}(s/w, w(\tau-z))dwdz, \tag{58}$$

where $A_{x\psi}(s,\tau)$ is the wideband crossambiguity function defined by

$$A_{x\psi}(s,\tau) = s\left|\int_{-\infty}^{\infty} x(t)\psi^*(s(t-\tau))dt\right|^2 = |\phi_x(s,\tau)|^2. \tag{59}$$

Derivation: In a channel that spreads a signal in both time and Doppler, the output is composed of time shifted and Doppler shifted replicas of the input signal. For a channel composed of a finite number of scatterers, the output signal would be given by

$$y(t) = \sum_{i=1}^{N} \rho_i\sqrt{s_i}\, x(s_i(t-\tau_i)), \tag{60}$$

where ρ_i is the random complex reflection coefficient of the ith scatterer. By Theorem 1, we know that the wavelet transform of an input signal dilated by an amount s_i and delayed an amount τ_i is given by

$$\mathcal{W}\{x(s_i(t-\tau_i))\} = \phi_x(s/s_i, s_i(t-\tau_i)). \tag{61}$$

Thus, by linearity, the wavelet transform of output signal in Eq. (60) is

$$\mathcal{W}\{y(t)\} = \phi_y(s,\tau) = \sum_{i=1}^{N} \rho_i\phi_x(s/s_i, s_i(\tau-\tau_i)). \tag{62}$$

If we assume that the expressions in Eqs. (60) and (62) are approximations for a channel described by a continuous distribution of scatterers, then as $N \to \infty$, we have

$$\phi_y(s,\tau) = \int_{z=-\infty}^{\infty}\int_{w=0}^{\infty} S(z,w)\phi_x(s/w, w(\tau-z))dwdz, \tag{63}$$

where $S(s,\tau)$ is called the *spreading function*, and describes the distribution of the reflection coefficient in range delay τ and Doppler variable s [7]. It is a stochastic function. Furthermore, assume that the channel exhibits uncorrelated spreading, then

$$E\{S(s,\tau)S^*(\hat{s},\hat{\tau})\} = R(s,\tau)\delta(s-\hat{s})\delta(\tau-\hat{\tau}), \tag{64}$$

where $\delta(\cdot)$ denotes the Dirac delta function. We apply Eq. (64) to the correlation function of the wavelet transform of the channel output as follows:

$$\begin{aligned} E\{\phi_y(s,\tau)\phi_y^*(\hat{s},\hat{\tau})\} &= \int_{z=-\infty}^{\infty}\int_{w=0}^{\infty}\int_{\hat{z}=-\infty}^{\infty}\int_{\hat{w}=0}^{\infty} \\ &\qquad E\{S(w,z)S^*(\hat{w},\hat{z})\} \\ &\qquad\quad \phi_x(s/w, w(\tau-z))\phi_x^*(\hat{s}/\hat{w}, \hat{w}(\hat{\tau}-\hat{z})) \\ &\qquad\quad\quad d\hat{w}dwd\hat{z}dz. \\ &= \int_{z=-\infty}^{\infty}\int_{w=0}^{\infty} \\ &\qquad R(w,z)\phi_x(s/w, w(\tau-z))\phi_x^*(\hat{s}/w, w(\hat{\tau}-z))dwdz. \end{aligned} \tag{65}$$

Setting $\hat{s} = s$ and $\hat{\tau} = \tau$ yields Eq. (58).

5. THE WAVELET EXPANSION AND DUABECHIES WAVELETS

The transform discussed in the previous sections shows that for a suitable choice of $\psi(t)$, any function in $L^2(R)$ can be expressed as an integral sum of time-dilated and time-delayed wavelets. Note that this is not an orthogonal representation, since, in general, we do not have

$$\int_{-\infty}^{\infty} \psi(s_1(t-\tau_1))\psi^*(s_2(t-\tau_2))dt = 0, \quad \text{for all } s_1 \neq s_2 \text{ and } \tau_1 \neq \tau_2. \tag{66}$$

Thus, the transformation is in some sense redundant. However, an orthogonal representation can be derived, provided the wavelet $\psi(t)$ obeys some additional restrictions. The result is an expansion composed of a countable sum of wavelets.

The description of this expansion was first given by Mallat [5]. In his work, he presented the concept of a *multiresolution approximation* of any function $g(t) \in L^2(R)$. This is a nested sequence of closed subspaces in $L^2(R)$ denoted as $\{V_j\}_{j\in Z}$, where Z is the set of all integers for which the following are true:

(a) $V_j \subset V_{j+1}$, for all $j \in Z$,

(b) $\bigcup_{j\in Z} V_j$ is dense in $L^2(R)$ and $\bigcap_{j\in Z} V_j = \emptyset$,

(c) $g(t) \in V_j \Leftrightarrow g(2t) \in V_{j+1}$ for all $j \in Z$

(d) $g(t) \in V_j \Rightarrow g(t - 2^{-j}k) \in V_j$ for all $j \in Z$

(e) Let $l^2(Z)$ denote the space of square summable infinite sequences, then there exists an isomorphism $T : V_0 \rightarrow l^2(Z)$ which commutes with the action of Z.

Properties (a) and (b) merely state that the nested sequence of subspaces must span the space $L^2(R)$. Properties (c) and (d) describe the effects of time dilation and time delay. Collectively, however, all the properties can be used to prove that there exists a function $\theta(t) \in L^2(R)$ such that for any $j \in Z$ the subspace V_j is spanned by the set $\{\sqrt{2^j}\theta(2^j(t-k))\}_{k\in Z}$. $\theta(t)$ is called the *scaling function*, and the properties stated above imply that if we wish to approximate (in a minimum integral square error sense) the function $g(t)$ by a function $g_j(t)$ in the subspace V_j, then

$$g_j(t) = \sum_{k=-\infty}^{\infty} g_{j,k}\, \sqrt{2^j}\theta(2^j(t - 2^{-j}k)), \tag{67}$$

where the coefficients of the expansion are given by

$$g_{j,k} = \sqrt{2^j} \int_{-\infty}^{\infty} g(t)\theta^*(2^j(t - 2^{-j}k))dt. \tag{68}$$

This, of course, is reminiscent of a generalized Fourier expansion; however, the difference here is that the expansion is only over the subspace V_j not the entire space $L^2(R)$. Equation (67) explains property (e) in that the sequence $\{g_{j,k}\}_{k\in Z}$ is an alternate representation of $g(t)$. Because the set $\{\sqrt{2^j}\theta(2^j(t-k))\}_{k\in Z}$ is a basis, the elements are orthogonal. Thus, by calculating $\|g\|_2^2$ one finds that it is equal to the sum of the squares of the sequence $\{g_{j,k}\}_{k\in Z}$. Since $g(t) \in L^2(R)$, $\|g\|_2^2$ is finite implying $\{g_{j,k}\}_{k\in Z} \in l^2(R)$.

For practical applications, we need to know more than just the existence of the scaling function; we need to know how it is parameterized, and how to compute it. A step in this direction is the following theorem that is proved in Refs. 2 and 5.

Theorem 6: Let $\theta(t)$ be a scaling function, and $H(f)$ be the Fourier series defined by

$$H(f) = \sum_{k=-\infty}^{\infty} h(k)e^{-j2\pi kf}, \tag{69}$$

where $\{h(k)\}_{k\in Z}$ is the sequence defined by

$$h(k) = \frac{1}{2}\int_{-\infty}^{\infty} \theta(2^{-1}t)\theta^*(t+k)dt. \tag{70}$$

Then $H(f)$ satisfies the following properties:

(i) $|H(0)| = 1$,

(ii) $h(k) \sim O(k^2)$ as $k \to \infty$,

(iii) $|H(f)|^2 + |H(f + 1/2)|^2 = 1$.

Furthermore, let

$$|H(f)| \neq 0 \quad \text{for} \quad f \in [0, 1/2), \tag{71}$$

then the Fourier transform of the scaling function is given by

$$\Theta(f) = \prod_{p=1}^{\infty} H(2^{-p} f). \tag{72}$$

The proof exploits properties (a) through (e), which define the multiresolution approximation. In particular, it uses properties (c) to say that the function $\theta(t/2)/2$ is equal to a weighted sum of the functions $\theta(t + k)$, and the weights are the elements of the sequence $\{h(k)\}_{k \in Z}$. Furthermore, any sequence used to define $H(f)$ in Eq. (69) so that $H(f)$ obeys properties (i) through (iii) of the theorem can be used to find $\theta(t)$ by defining its Fourier transform through Eq. (72). Thus, our choice of the $h(k)$'s is somewhat arbitrary.

The expansion given by Eq. (67) is simple, but not always convenient for practical applications. For, if we wanted the approximation of $g(t)$ in the subspace V_j and had the expansion for the approximation in V_{j-1}, we would have to recompute all expansion coefficients. Furthermore, this expansion does not lend itself to defining filtering operations. An alternate expansion can be derived by noting (through the projection theorem) that there exists a subspace O_j composed of functions that are orthogonal to those composing V_j such that

$$O_j \bigoplus V_j = V_{j+1}, \tag{73}$$

where $\bigoplus$ denotes the Cartesian product. Thus, from property (b) of the multiresolution expansion one can show that

$$\bigcup_{j \in Z} O_j = L^2(R), \tag{74}$$

In light of this new definition we have the following theorem whose proof can be found in the Refs. 2 and 5.

Theorem 7: Let $\{V_j\}_{j \in Z}$ define the multiresolution approximation of the space $L^2(R)$, $\theta(t)$ be the scaling function whose Fourier transform is $\Theta(f)$, and $H(f)$ be the Fourier series describing the Fourier transform of $\theta(t)$ as in Theorem 6. Then there exists a function $\psi(t)$ such that $\{\sqrt{2^j}\psi(2^j(t - 2^{-j}k))\}_{j,k \in Z \times Z}$ is a basis for $L^2(R)$, and the Fourier transform of $\psi(t)$ is given by

$$\Psi(f) = K\left(\frac{f}{2}\right)\Theta\left(\frac{f}{2}\right), \tag{75}$$

where

$$K(f) = e^{-j2\pi f} H^*(f + 1/2). \tag{76}$$

From Eqs. (75) and (76) it is possible to show that $\theta(t)$ is equal to a linear sum of time delayed scaling functions. The function $\psi(t)$ is called an orthogonal wavelet, and the theorem given above says that any function $g(t)$ in $L^2(R)$ can be written as

$$g(t) \overset{a.e.}{=} \sum_{j,k \in Z \times Z} g_{j,k} \sqrt{2^j}\psi(2^j(t - 2^{-j}k)), \tag{77}$$

where

$$g_{j,k} = \sqrt{2^j} \int_{-\infty}^{\infty} g(t)\psi^*(2^j(t - 2^{-j}k))dt = \phi_g(2^j, 2^{-j}k). \tag{78}$$

Thus, we see that the wavelet expansion coefficients are equal to the value of the wavelet transform at the points $(s, \tau) = (2^j, 2^{-j}k)$. Figure 1 shows this. Moreover, we see that $\theta(t)$ plays a role in the definition of $\psi(t)$. From a computational standpoint, Theorem 7 says that we must find $\theta(t)$ (or its Fourier transform) first, and then compute $\psi(t)$.

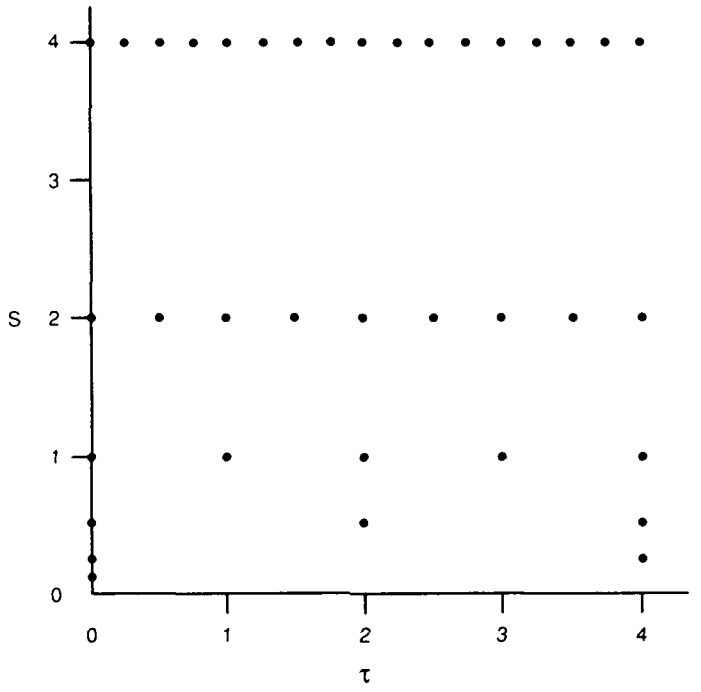

Fig. 1 — Points in the (s, τ) plane where the wavelet expansion coefficients are equal to the wavelet transform. This figure shows all points lying within and on the boundary of the region $s \in [2^{-3}, 2^2]$ and $\tau = [0, 4]$.

Theorems 6 and 7 not only suggest how the scaling function and orthogonal wavelets can be computed, but also suggest that we can, to some degree, control the shape of the wavelet in the time domain according to how we choose the sequence $\{h(k)\}_{k \in Z}$. One desirable property is to have a wavelet with compact support in the time domain, i.e., it is time limited in that it is nonzero only over a given interval. Such a wavelet gives a true sense of time locality. A set of orthogonal wavelets with compact support was discovered by Daubechies [2]. They are parameterized by an integer n, are real valued, and are denoted as $\psi_n(t)$ for $n \geq 2$. In fact,

$$supp\ \psi_n \subset [(1-n), n], \tag{79}$$

and

$$\int_{-\infty}^{\infty} \psi_n(2^i(t - 2^{-i}l)\psi_n^*(2^j(t - 2^{-j}k))dt = 0 \quad \text{for all } l \neq k \text{ or } i \neq j. \tag{80}$$

The associated scaling function is denoted by $\theta_n(t)$. These wavelets are derived by choosing the sequence $\{h(k)\}_{k\in Z}$ so that is of finite length (a FIR filter in signal processing parlance). The result is the set of sequences $\{h_n(k)\}_{k\in Z}$ that are nonzero for $k = 0, 1, \ldots, (2n-1)$; thus, they are of length $2n$. Details of the procedure for finding these sequences can be found in Daubechies' original paper; however, we have tabulated the sequences for $n = 2, 3, \ldots, 14$ in the appendix.

Figure 2 shows the Daubechies orthogonal wavelets for $n = 2, 3, \ldots, 13$ They were generated by first calculating (approximating) the Fourier transform of the associated scaling function via the equation

$$\Theta_n(f) = \prod_{p=0}^{P} H_n(2^{-p}f), \tag{81}$$

where

$$H_n(f) = \sum_{k=0}^{2n-1} h_n(k) e^{-j2\pi kf}. \tag{82}$$

Once $\Theta_n(f)$ is found, we calculate the Fourier transform of the orthogonal wavelet as

$$\Psi_n(f) = K_n\left(\frac{f}{2}\right)\Theta_n\left(\frac{f}{2}\right), \tag{83}$$

where

$$K_n(f) = e^{-j2\pi f} H_n^*(f + 1/2). \tag{84}$$

Equations (81-84) follow directly from Eq. (69), (72), (75), and (76). In particular, the truncated product in Eq. (81) gives good results for $P = 20$ for low values of n ($n = 3$), to $P = 25$ for high values of n ($n = 13$). This was checked by calculating the normalized cross correlation between two Daubechies wavelets of order n, where one was derived by using $P = N$, and the other with $P = N + 1$. For $P = 25$ (or $P = 20$ for low values of n) the correlation was negligibly different from 1.

6. PROPERTIES OF DAUBECHIES WAVELETS

We now state and prove five theorems about the Daubechies wavelets introduced in the previous section. The first three theorems state that these wavelets are bounded, continuous, and in most cases differentiable.

Theorem 8: $\psi_n(t)$ is bounded for all n.

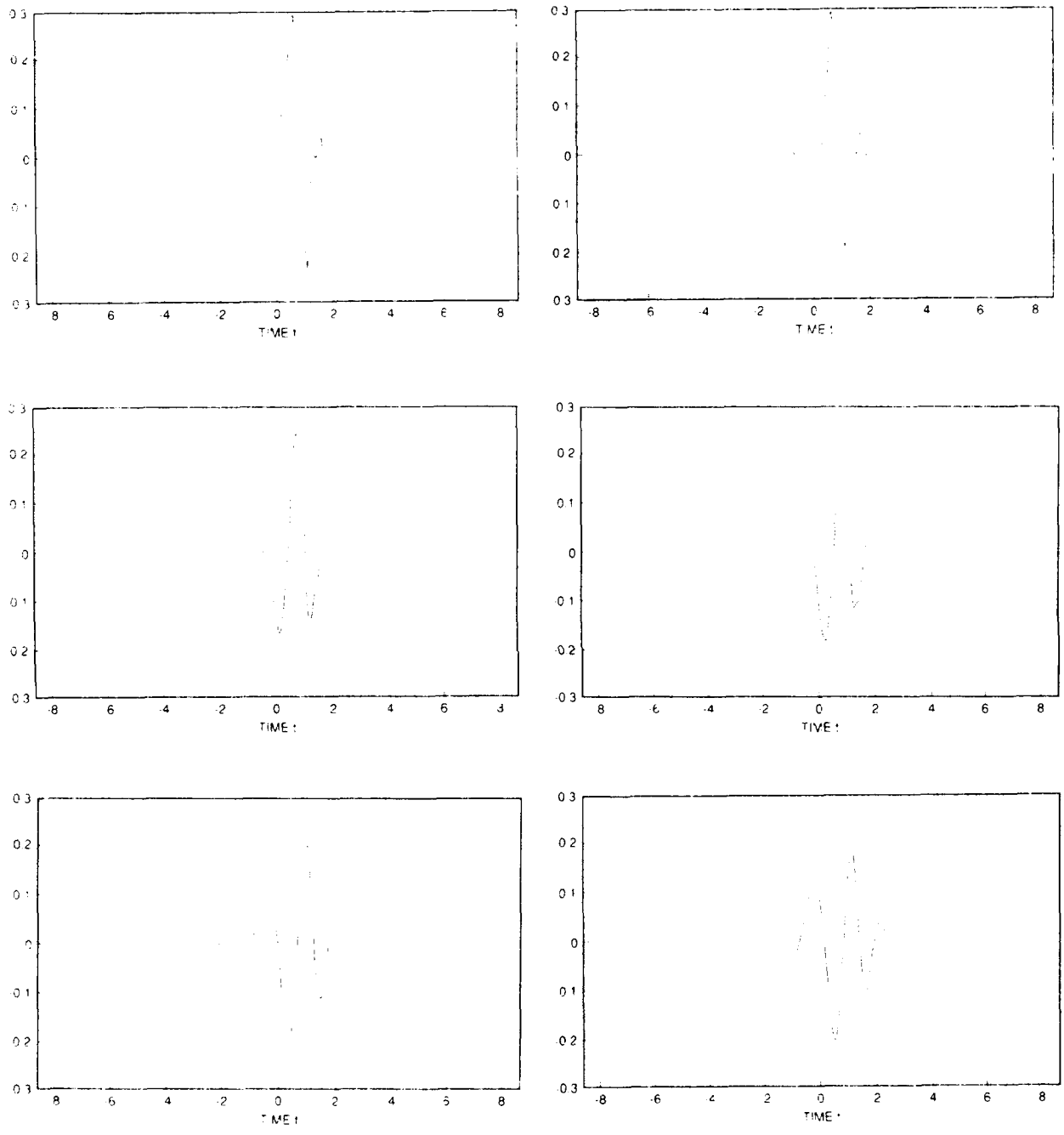

Fig. 2a -- Daubechies orthogonal wavelets for $n = 2, \ldots, 7$. These wavelets are nonzero only in the interval $[(1 - n), n]$.

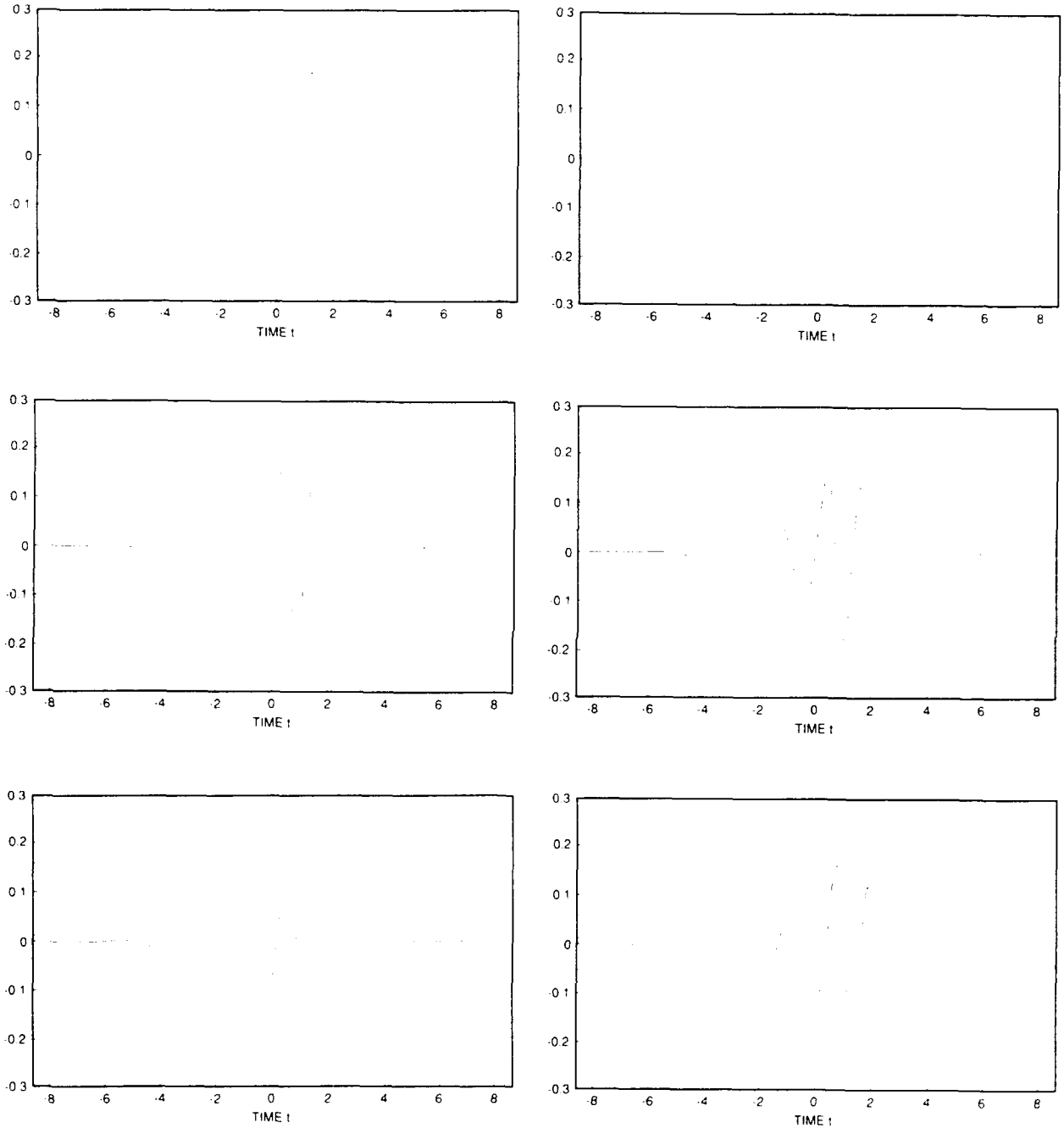

Fig. 2b — Daubechies orthogonal wavelets for $n = 8, \ldots, 13$. These wavelets are nonzero only in the interval $[(1 - n), n]$.

Proof of Theorem 8: Daubechies showed that the Fourier transform of the wavelet $\psi_n(t)$ has the property

$$|\Theta_n(f)| \leq C(1+|f|)^{-n+\log B/\log 2} \leq C < \infty, \tag{85}$$

for some constant C, and where $B < 2^{n-1}$. It follows that

$$\begin{aligned} |\theta_n(t)| &= \left| \int_{-\infty}^{\infty} \Theta_n(f) e^{j2\pi ft} df \right| \\ &\leq \int_{-\infty}^{\infty} |\Theta_n(f)| df \\ &\leq C \int_{-\infty}^{\infty} \frac{df}{(1+|f|)^{n-\log B/\log 2}}, \end{aligned} \tag{86}$$

and

$$\frac{\log B}{\log 2} < n-1 \Rightarrow n - \frac{\log B}{\log 2} > 1. \tag{87}$$

Therefore, there exists some $\epsilon > 0$ such that Eq. (86) can be rewritten to yield

$$\begin{aligned} |\theta_n(t)| &\leq C \int_{-\infty}^{\infty} \frac{df}{(1+|f|)^{1+\epsilon}} \\ &= 2C \int_0^{\infty} \frac{df}{(1+f)^{1+\epsilon}} \\ &= 2C \int_1^{\infty} \frac{dz}{z^{1+\epsilon}} \\ &= -2C \frac{z^{-\epsilon}}{\epsilon}\Big|_1^{\infty} \\ &= \frac{2C}{\epsilon} < \infty. \end{aligned} \tag{88}$$

Thus, the scaling function $\theta_n(t)$ is bounded for all t. Since $\{h_n(k)\}_{k\in Z}$ is a finite sequence, it is possible to show through Eqs. (81) and (82) that $\psi_n(t)$ is a finite sum of time delayed scaling functions. Therefore, the wavelet $\theta_n(t)$ is bounded for all t.

Theorem 9: $\psi_n(t)$ is continuous for all n.

Proof of Theorem 9: Let $C^{\alpha}(R)$ be the set of all functions such that

$$g(t) \in C^{\alpha}(R) \Leftrightarrow \int_{-\infty}^{\infty} |G(f)|(1+|f|)^{1+\alpha} < \infty. \tag{89}$$

If $\alpha = k$ for $k = 0, 1, 2, \ldots$, then $C^k(R)$ is the space of k-times continuously differentiable functions, where, in particular, $C^0(R)$ is the space of continuous functions. Daubechies has already shown that $\psi_n(t) \in C^{\alpha}(R)$ for some $\alpha > 0$. Thus, we only need to establish that this implies $\psi(t) \in C^0(R)$. To begin, note that for any $\epsilon \in [0, \alpha]$,

$$(1+|f|)^{1+\epsilon} \leq (1+|f|)^{1+\alpha}, \text{ for all } f. \tag{90}$$

This implies that

$$|G(f)|(1+|f|)^{1+\epsilon} \leq |G(f)|(1+|f|)^{1+\alpha}, \text{ for all } f, \tag{91}$$

which, in turn, implies

$$\int_{-\infty}^{\infty} |G(f)|(1+|f|)^{1+\epsilon} df \leq \int_{-\infty}^{\infty} |G(f)|(1+|f|)^{1+\alpha} df < \infty. \tag{92}$$

Thus, by the definition of $C^{\alpha}(R)$ as it follows from Eq. (89), we see that $\phi_n(t) \in C^{\epsilon}(R)$ for all $\epsilon \in [0, \alpha]$. Therefore, $\psi_n(t) \in C^0(R)$, and so $\psi_n(t)$ is continuous.

Theorem 10: $\psi_n(t)$ is continuously differentiable for $n \geq 4$.

Proof of Theorem 10: Daubechies proved that $\alpha > 1$ for $n \geq 4$. Furthermore, from the proof of the previous theorem, we know that $\psi_n(t) \in C^{\epsilon}$ for all positive ϵ less than α. Thus, $\psi_n(t) \in C^1(R)$ for all $n \geq 4$. In other words, $\psi_n(t)$ is continuously differentiable for $n \geq 4$.

Theorem 11: For $n \geq 4$, $\psi_n(t)$ has a finite spectral variance, i.e.,

$$\int_{-\infty}^{\infty} f^2 |\Psi_n(f)| df < \infty. \tag{93}$$

Proof of Theorem 11: For $n \geq 4$, $\psi_n(t)$ is continuously differentiable, therefore, $\psi_n'(t)$ is continuous. Also, since $\psi_n(t)$ has compact support (an interval), so does $\psi_n'(t)$. Furthermore, since a continuous function over a compact interval is bounded, we see that $\psi_n'(t)$ is bounded over $supp\ \psi_n$, thus

$$\begin{aligned} \int_{-\infty}^{\infty} |\psi_n'(t)|^2 dt &= \int_{supp\ \psi_n} |\psi_n'(t)|^2 dt \\ &\leq meas(supp\ \psi_n) \cdot \max_{supp\ \psi_n} |\psi_n'(t)|^2 \\ &\leq meas([(1-n), n]) \cdot \max_{t \in [(1-n), n]} |\psi_n'(t)|^2 \\ &= (2n-1) \cdot \max_{t \in [(1-n), n]} |\psi_n'(t)|^2 < \infty, \end{aligned} \tag{94}$$

where $meas(\cdot)$ is the Lebesgue measure, and have used Eq. (79). Since the Fourier transform of $\psi_n'(t)$ is $\jmath 2\pi f \Psi_n(f)$, we have by Parseval's Theorem,

$$4\pi^2 \int_{-\infty}^{\infty} f^2 |\Psi(f)|^2 df = \int_{-\infty}^{\infty} |\psi_n'(t)|^2 dt < \infty. \tag{95}$$

Theorem 12: For $n \geq 4$, or for any wavelet with a finite spectral variance, if $g(t) \in L^2(R)$, then

$$\left|\frac{\partial \phi_g(s,\tau)}{\partial \tau}\right|^2 \rightarrow 0, \text{ as } s \rightarrow 0. \tag{96}$$

Proof of Theorem 12: By the definition of the wavelet transform we have

$$\begin{aligned}\frac{\partial \phi_g(s,\tau)}{\partial \tau} &= \sqrt{s}\frac{\partial}{\partial \tau}\int_{-\infty}^{\infty} g(t)\psi_n^*(s(t-\tau))dt \\ &= -s^{3/2}\int_{-\infty}^{\infty} g(t)\psi_n^{*\prime}(s(t-\tau))dt. \end{aligned}\tag{97}$$

Therefore, taking the square magnitude of Eq. (97), applying the Schwartz inequality, and using Eq. (95) from Theorem 11, we have

$$\begin{aligned} 0 \leq \left|\frac{\partial \phi_g(s,\tau)}{\partial \tau}\right|^2 &= s^3\left|\int_{-\infty}^{\infty} g(t)\psi_n^{*\prime}(s(t-\tau))dt\right|^2 \\ &\leq s^3\int_{-\infty}^{\infty}|g(t)|^2dt\int_{-\infty}^{\infty}|\psi_n^{*\prime}(s(t-\tau))|^2dt \\ &= s^2\int_{-\infty}^{\infty}|g(t)|^2dt\int_{-\infty}^{\infty}|\psi_n^{*\prime}(z)|^2dz \\ &= (2\pi s)^2\|g\|_2^2\int_{-\infty}^{\infty} f^2|\Psi_n(f)|^2df < \infty. \end{aligned}\tag{98}$$

Thus, by applying the squeeze theorem for limits, Eq. (96) follows from Eq. (98). This proves the theorem.

Basically, this theorem says that as s approaches zero, the derivative of the wavelet transform along the τ axis approaches zero. In other words, $\phi(s,\tau)$ becomes 'smoother' along τ as $s \rightarrow 0$.

Theorem 13: $\psi_n(t) \in L^1(R) \bigcap L^2(R)$ for all n.

Proof of Theorem 13: By Theorem 8 we know that $\psi_n(t)$ is bounded, i.e., $|\psi_n(t)| \leq K$ for some $K < \infty$. Therefore, using Eq. (79) we have

$$\int_{-\infty}^{\infty}|\psi_n(t)|dt \leq meas\ (supp\ \psi_n)\cdot K \leq (2n-1)\cdot K < \infty, \tag{99}$$

which implies that $\psi_n(t) \in L^1(R)$. Also,

$$\int_{-\infty}^{\infty}|\psi_n(t)|^2dt \leq meas\ (supp\ \psi_n)\cdot K^2 \leq (2n-1)\cdot K^2 < \infty, \tag{100}$$

which implies that $\psi_n(t) \in L^2(R)$. This proves the theorem.

This last theorem shows that the Daubechies orthogonal wavelets obey the regularity property as defined in Eq. (9). This says that the wavelet transform that uses a Daubechies orthogonal wavelet as the transform kernel is meaningful in the sense that its inverse exists.

Theorem 14: For all Daubechies wavelets, the following are true:

$$\text{(i)} \quad \lim_{f\to 0} \frac{|\Psi_n(f)|^2}{|f|} = 0,$$

$$\text{(ii)} \quad \lim_{f\to 0} |\Psi_n(f)|^2 = 0,$$

$$\text{(iii)} \quad \int_{-\infty}^{\infty} \frac{|\Psi_n(f)|^2}{|f|} df < \infty.$$

Proof of Theorem 14: Daubechies and Mallat have shown that

$$\Psi_n(f) = e^{-j2\pi f} H_n^*(f + 1/2) \prod_{k=1}^{\infty} H_n(f/2^k), \tag{101}$$

where

$$H_n(f) = \left[(1 + e^{-j2\pi f})/2\right]^n Q_n(f), \tag{102}$$

and

$$|Q_n(f)|^2 = \sum_{k=0}^{n-1} \binom{n-1+k}{k} sin^{2k}(\pi f). \tag{103}$$

From Eqs. (102) and (103) one finds

$$\lim_{f\to 0} |H_n(f)|^2 = 1, \tag{104}$$

which implies

$$\lim_{f\to 0} \left| \prod_{k=1}^{\infty} H_n(f/2^k) \right|^2 = 1. \tag{105}$$

Now consider the limit

$$\lim_{f\to 0} \frac{|H_n(f+1/2)|^2}{|f|} = \lim_{f\to 0} \left| \frac{(1 - e^{-j\pi f})}{2} \right|^{2n} \cdot \lim_{f\to 0} \frac{|Q_n(f+1/2)|^2}{|f|}. \tag{106}$$

Using Eq. (103), and L'Hôpital's rule, we see that

$$\begin{aligned} \lim_{f\to 0^+} \frac{|Q_n(f+1/2)|^2}{|f|} &= \lim_{f\to 0^+} \frac{D_f |Q_n(f+1/2)|^2}{D_f f} \\ &= 2\pi \lim_{f\to 0^+} \sum_{k=1}^{n-1} k \binom{n-1+k}{k} sin^{2k-1}(\pi f + \pi/2) cos(\pi f + \pi/2) \\ &= 0. \end{aligned} \tag{107}$$

Similarly,

$$\lim_{f\to 0^-} \frac{|Q_n(f+1/2)|^2}{|f|} = 0. \tag{108}$$

Combining Eqs. (101-108) yields

$$\begin{aligned}
\lim_{f\to 0} \frac{|\Psi_n(f)|^2}{|f|} &= \lim_{f\to 0} \frac{|H_n(f+1/2)|^2}{|f|} \cdot \lim_{f\to 0} \left| \prod_{k=1}^{\infty} H_n(\pi f/2^k) \right|^2 \\
&= \lim_{f\to 0} \left| \frac{(1-e^{-j2\pi f})}{2} \right|^{2n} \cdot \lim_{f\to 0} \frac{|Q_n(f+1/2)|^2}{|f|} \cdot \lim_{f\to 0} \left| \prod_{k=1}^{\infty} H_n(f/2^k) \right|^2 \\
&= 0 \cdot 0 \cdot 1 = 0,
\end{aligned} \tag{109}$$

which proves (i). (ii) follows from (i) for, if $|\Psi_n(f)|^2 \to K \neq 0$ as $f \to 0$, then the limit in Eq. (109) would be infinite.

(iii) is proved in two parts, since we can write the integral in (iii) as

$$\int_{-\infty}^{\infty} \frac{|\Psi_n(f)|^2}{|f|} df = \int_{-1}^{1} + \int_{|f|\geq 1} \frac{|\Psi_n(f)|^2}{|f|} df = I_1 + I_2. \tag{110}$$

Consider I_1. We first note that because $|H_n(f)|^2 \leq 1$, and using Eq. (101), that

$$|\Psi_n(f)|^2 = |e^{-j2\pi f}|^2 |H_n(f+1/2)|^2 \left| \prod_{k=1}^{\infty} H_n(f/2^k) \right|^2 \leq |H_n(f+1/2)|^2. \tag{111}$$

Also, from Eqs. (102) and (103) we have

$$\begin{aligned}
|H_n(f)|^2 &= \left| \frac{1+e^{-j2\pi f}}{2} \right|^{2n} |Q_n(f)|^2 \\
&\leq \left| \frac{1+e^{j2\pi f}}{2} \right|^{2n} \max_{f\in[-1/2,1/2]} |Q_n(f)|^2 \\
&= \cos^{2n}(\pi f) \cdot \max_{f\in[-1/2,1/2]} |Q_n(f)|^2.
\end{aligned} \tag{112}$$

Therefore, since $sin(x) \leq |x|$, from Eq. (112) it follows that

$$\begin{aligned}
\frac{|H_n(f+1/2)|^2}{|f|} &\leq \left[\max_{f\in[-1/2,1/2]} |Q_n(f)|^2 \right] \frac{\cos^{2n}(\pi f + \pi/2)}{|f|} \\
&= \left[\max_{f\in[-1/2,1/2]} |Q_n(f)|^2 \right] \frac{sin^{2n}(\pi f)}{|f|} \\
&\leq \left[\max_{f\in[-1/2,1/2]} |Q_n(f)|^2 \right] \frac{(\pi f)^{2n}}{|f|} \\
&= \left[\max_{f\in[-1/2,1/2]} |Q_n(f)|^2 \right] \pi^{2n} |f|^{2n-1}.
\end{aligned} \tag{113}$$

Integrating both sides of Eq. (113) yields

$$I_1 = \int_{-1}^{1} \frac{|H_n(f+1/2)|^2}{|f|} df = \left[\max_{f \in [-1/2, 1/2]} |Q_n(f)|^2 \right] \pi^{2n} \int_{-1}^{1} |f|^{2n-1} df$$
$$= \left[\max_{f \in [-1/2, 1/2]} |Q_n(f)|^2 \right] \pi^{2n} \frac{1}{n} < \infty, \tag{114}$$

which proves that $I_1 < \infty$. Note that for $|f| \geq 1$,

$$\frac{|\Psi_n(f)|^2}{|f|} \leq |\Psi_n(f)|^2. \tag{115}$$

Since $\psi_n(t) \in L^2(R)$, by Parseval's Theorem we know that $\Psi_n(f) \in L^2(R)$, so it follows that

$$I_2 = \int_{|f| \geq 1} \frac{|\Psi_n(f)|^2}{|f|} df \leq \int_{-\infty}^{\infty} |\Psi_n(f)|^2 df < \infty. \tag{116}$$

Combining Eqs. (114) and (116) yields

$$\int_{-\infty}^{\infty} \frac{|\Psi_n(f)|^2}{|f|} df = I_1 + I_2 < \infty, \tag{117}$$

which proves (iii).

7. APPLICATION: WAVELET PASSBAND FILTERING

Frequently one must filter a passband signal to reduce transients or reject out of band signals. Generally, this is accomplished by passing the signal through an analog filter designed to pass only those frequency (Fourier) components that occupy the signal passband. This is equivalent to convolving the input signal with the impulse response of the filter. In this section, we show how filtering can also be accomplished by using the wavelet expansion.

It was shown in Section 5 that if $g(t) \in L^2(R)$ has the wavelet expansion

$$g(t) \stackrel{a.e.}{=} \sum_{j,k \in Z \times Z} g_{j,k} \sqrt{2^j} \psi(2^j(t - 2^{-j}k)), \tag{118}$$

where

$$g_{j,k} = \sqrt{2^j} \int_{-\infty}^{\infty} g(t) \psi^*(2^j(t - 2^{-j}k)) dt. \tag{119}$$

We realize, however, that the components of the expansion associated with large values of 2^j roughly correspond to short term features (transients) of the signal $g(t)$, and the components associated with small values of 2^j contribute to the long term (average or dc) components of $g(t)$. Thus, to do passband filtering in the wavelet domain, we can construct

a signal with a wavelet expansion that uses only those coefficients that correspond to a narrow range of dilations. In mathematical terms, we construct the signal

$$g_{bp}(t) = \sum_{j=j_l}^{j_h} \sum_{k \in Z} g_{j,k} \sqrt{2^j} \psi(2^j(t - 2^{-j}k)). \tag{120}$$

Thus, we are constructing a signal with the coefficients associated with the wavelets whose dilations are $2^{j_l}, \ldots, 2^{j_h}$.

We demonstrate this filtering method by the example that follows. Figure 3 shows a real valued signal composed of two windowed sine waves and a spike (transient). The uncontaminated signal is mathematically expressed as

$$g(t) = \frac{1}{2} exp\Big((t - \bar{t})^2/\sigma_1^2\Big)[sin(2\pi f_1 t) + sin(2\pi f_2 t)], \tag{121}$$

where $\bar{t} = 8.533$, $\sigma_1 = 3.413$, $f_1 = 1.5$ Hz, and $f_2 = 2f_1 = 3.0$ Hz. Whereas the spike is given by

$$n(t) = 3\, exp\Big((t - \bar{t})/\sigma_2^2\Big), \tag{122}$$

where $\sigma_2 = 0.071$. Figure 4 shows the Fourier spectrum of $g(t) + n(t)$, and Fig. 5 shows its wavelet transform. The vertical ridge in Fig. 5 is due to the transient. Clearly, the wavelet transform show the locality of the transient in time, which the Fourier spectrum does not. We first analog filter the signal in Fig. 3 by passing it through a Chebyshev passband filter whose Fourier spectrum is given by

$$C(f) = \frac{1}{S^4 + 1.80377S^3 + 2.62680S^2 + 2.02550S + 0.82851}, \tag{123}$$

where

$$S = \jmath 2\pi \frac{f^2 - f_0^2}{Bf}, \tag{124}$$

and $f_0 = \sqrt{f_h f_l}$ is the geometric mean of the filter passband whose width is $B = f_h - f_l$ where $f_l < f_h$. In this case, $f_l = 1.15$ Hz, and $f_h = 3.35$ Hz. The Fourier spectrum of the filter, shown in Fig. 6, displays some ripple in the passband. This is an inherent characteristic of the Chebyshev filter type [9]. For this particular filter, the ripple width (peak-to-peak difference) is 0.1 dB. Figure 7 shows the Chebyshev filter output in time in response to the signal in Fig. 3, and Fig. 8 shows its Fourier spectrum. In Fig. 7, we note two features. First, we see that as compared to the original function, the two sine waves are displaced in time. This is due to the phase characteristic of the filter: each sinewave experiences a different phase shift. Second, we see that the entire signal is displaced in time slightly, thus accounting for a group delay that is also due to the phase characteristic of the filter.

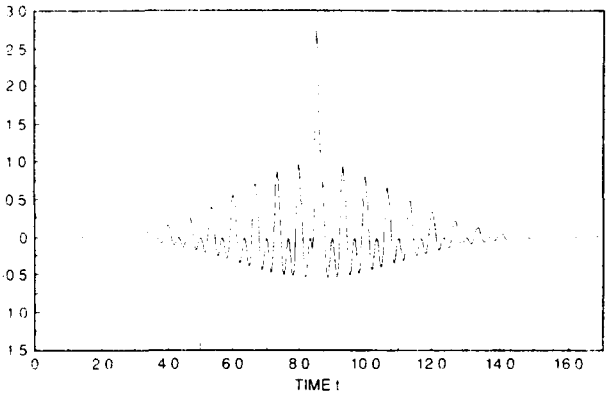

Fig. 3 — Real valued input signal composed of two windowed sine waves and a spike

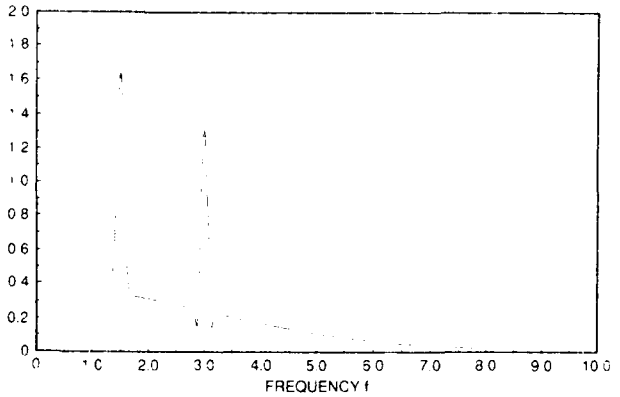

Fig. 4 — Square magnitude of the input signal's Fourier spectrum

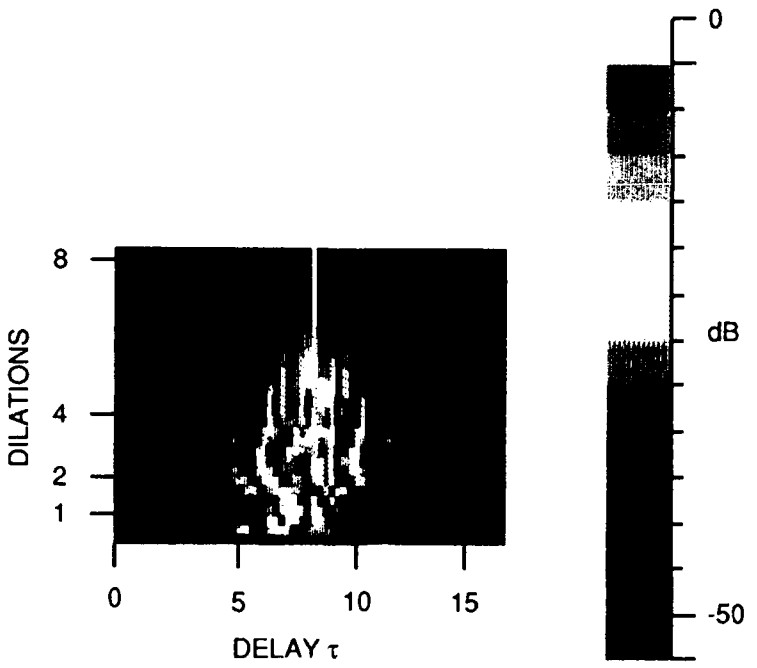

Fig. 5 — Square magnitude of the input signal's wavelet transform. The transform kernel is a Daubechies orthogonal wavelet of order $n = 8$

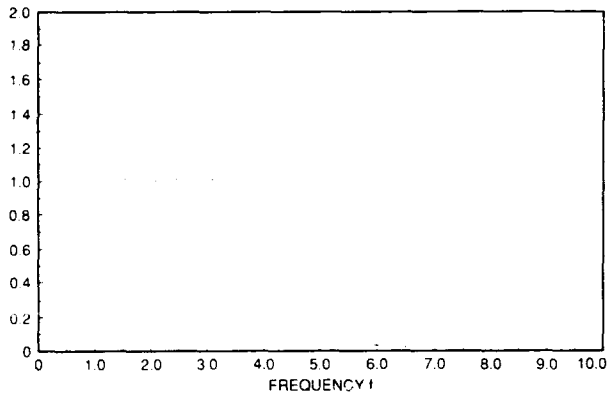

Fig. 6 — Square magnitude of the Chebyshev passband filter's Fourier spectrum

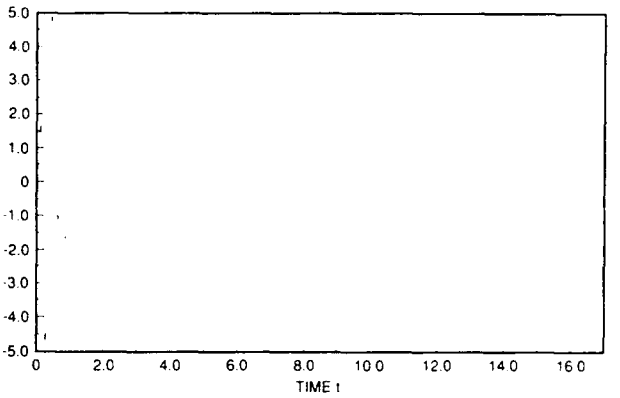

Fig. 7 — Output of the Chebyshev passband filter in time in response to the signal in Fig. 3

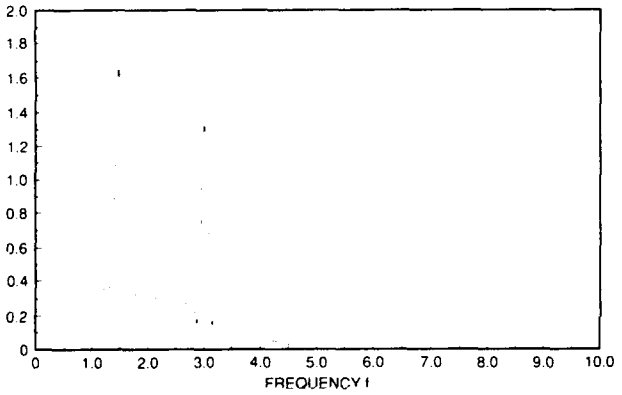

Fig. 8 — Square magnitude of the Fourier spectrum of the input signal after analog filtering with a Chebyshev passband filter

Figures 9 and 10 show the result of applying the wavelet filtering method to the signal. Figure 9 shows the result for a reconstruction using dilations 2^1, 2^2, and 2^3. Figure 10 shows a reconstruction using slightly less wavelet bandwidth. In this case, we have used dilations 2^1 and 2^2. As compared to passing the signal through a Chebyshev filter, we see qualitatively that wavelet filter produced more amplitude distortion in the time domain but does not show the same effect of phase distortion or group delay. Both analog filtering (using the Chebyshev filter) and wavelet filtering de-emphasize the spike but do not completely remove it.

Figures 11 and 12 show the Fourier spectrum of the signals derived through wavelet filtering. They show that the low frequency components of the spectrum have been removed, and this is reasonable since a large part of the spectral energy of the spike is located there. Furthermore, we see that in Fig. 12 a spurious peak occurs, which implies that wavelet filtering causes nonlinear distortion in the Fourier frequency domain. Figures 13 to 15 show the wavelet transforms of the signals resulting from wavelet filtering, and by analog filtering. (Remember that the wavelet expansion coefficients of these functions are equal to their wavelet transforms at the points $(s,\tau) = (2^i, 2^{-i}k)$ for $i,k \in Z \times Z$.) As compared to the wavelet transform of the input signals shown in Fig. 5, these figures show a reduction of the ridge in the (s,τ) plane associated with the spike.

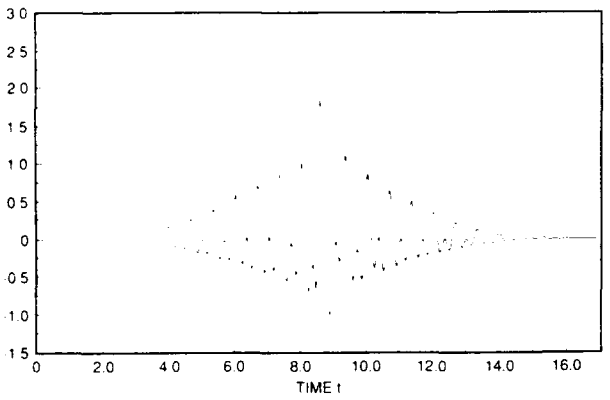

Fig. 9 — Wavelet reconstruction of the input signal using dilations 2^1, 2^2, and 2^3. The wavelet expansion used the Daubechies orthogonal wavelet of order $n = 8$.

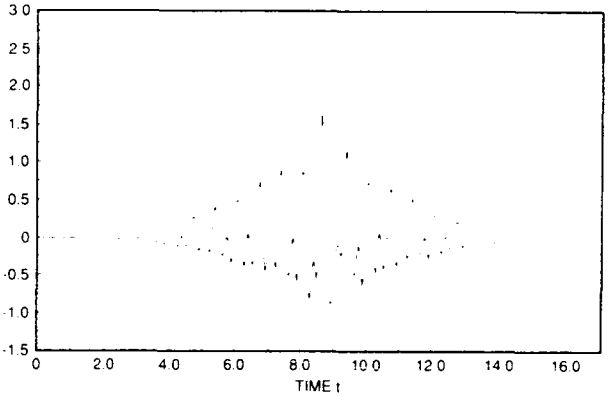

Fig. 10 — Wavelet reconstruction of the input signal by using dilations 2^1 and 2^2. The wavelet expansion used the Daubechies orthogonal wavelet of order $n = 8$.

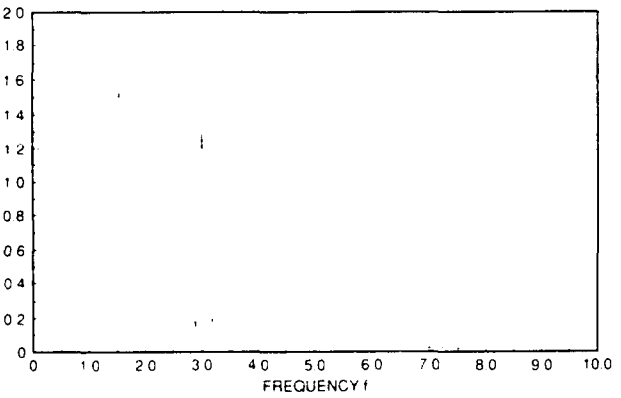

Fig. 11 — Fourier spectrum (square magnitude) of the wavelet reconstruction of the input signal using dilations 2^1, 2^2, and 2^3. The wavelet expansion used the Daubechies orthogonal wavelet of order $n = 8$.

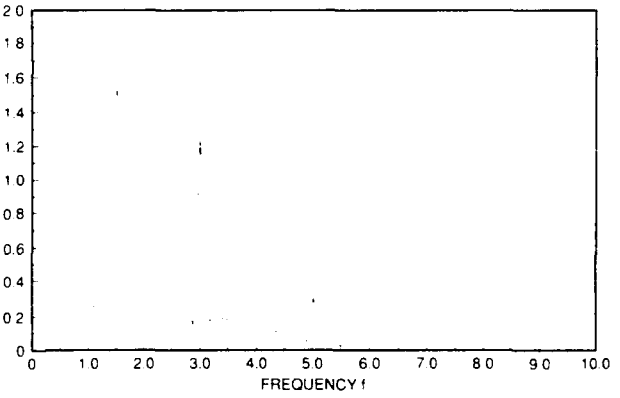

Fig. 12 — Fourier spectrum (square magnitude) of the wavelet reconstruction of the input signal using dilations 2^1 and 2^2. The wavelet expansion used the Daubechies orthogonal wavelet of order $n = 8$.

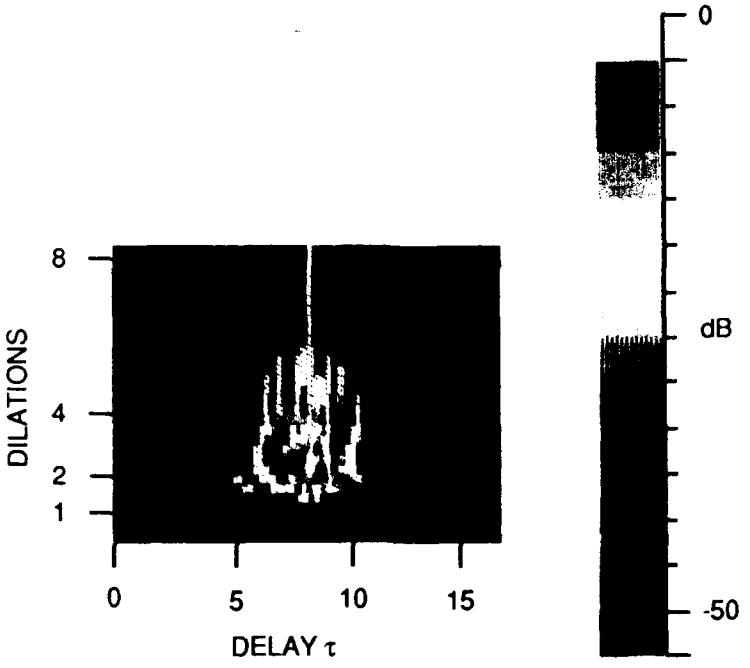

Fig. 13 — Wavelet transform (square magnitude) of the wavelet reconstruction of the input signal using dilations 2^1, 2^2, and 2^3. The transform kernel is a Daubechies orthogonal wavelet of order $n = 8$.

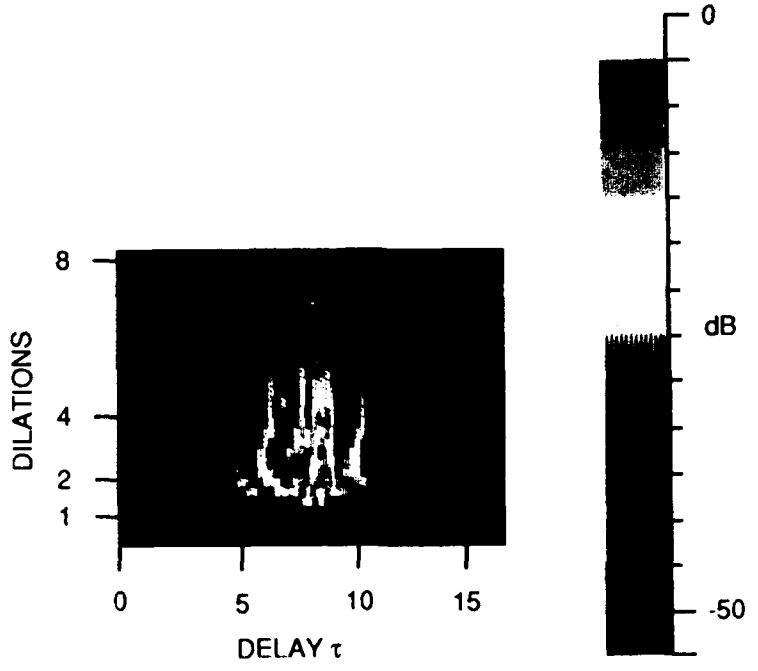

Fig. 14 — Wavelet transform (square magnitude) of the wavelet reconstruction of the input signal using dilations 2^1 and 2^2. The transform kernel is a Daubechies orthogonal wavelet of order $n = 8$.

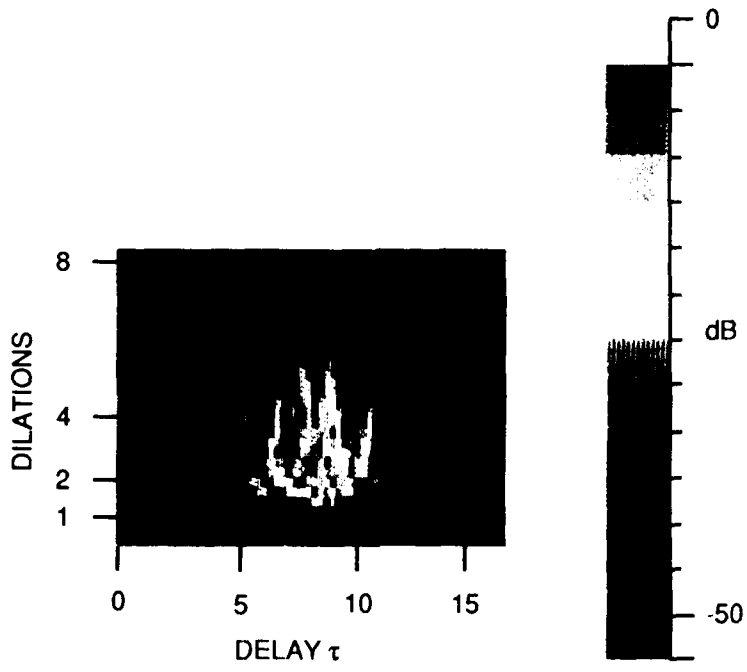

Fig. 15 — Square magnitude of the wavelet transform of the input signal after analog filtering with a Chebyshev passband filter. The transform kernel is a Daubechies orthogonal wavelet of order $n = 8$.

8. APPLICATION: A DECONVOLUTION ALGORITHM

The deconvolution of two signals has important applications in geophysics and communication systems. The problem can be simply stated as follows: given a known input signal $x(t)$ driving a linear system whose unknown impulse response is $g(t)$, estimate $g(t)$ given the known (measured) output signal $y(t) = x(t) * g(t)$.

The easiest way to deconvolve is to simply calculate the Fourier transforms $X(f)$ and $Y(f)$, and find their quotient $G(f) = Y(f)/X(f)$. This is reasonable in principle but in practice can produce numerically unstable results, since one may have to divide $Y(f)$ by a very small $X(f)$ if our discrete numerical approximation of $X(f)$ brings us close to one of its zeros. This problem may become worse in the presence of noise in the measurement of $X(f)$. The following outlines a deconvolution procedure in the context of the wavelet expansion.

Both the impulse response $g(t)$ and the output $y(t)$ have wavelet expansions given by

$$\begin{aligned} g(t) &\overset{a.e.}{=} \sum_{i,n \in Z \times Z} g_{i,n} \psi(2^i(t - n2^{-i})), \\ y(t) &\overset{a.e.}{=} \sum_{j,m \in Z \times Z} y_{j,m} \psi(2^j(t - m2^{-j})), \end{aligned} \tag{125}$$

where as compared to the definition in Eq. (77) we have dropped the factors $\sqrt{2^i}$ and $\sqrt{2^j}$ inside the summations for notational convenience, i.e., $g_{i,n}\ \sqrt{2^i} \rightarrow g_{i,n}$ and $y_{j,m}\ \sqrt{2^j} \rightarrow y_{j,m}$. The coefficients $g_{i,n}$ are unknown; they are the ones we wish to estimate. On the other hand, the coefficients $y_{j,m}$ are known and are calculated by the direct application of Eq. (78) on the known (measured) output $y(t)$. We also know that

$$\begin{aligned} y(t) &= x(t) * g(t) \\ &= x(t) * \sum_{i,n \in Z \times Z} g_{i,n} \psi(2^i(t - n2^{-i})) \\ &= \sum_{i,n \in Z \times Z} g_{i,n}\ x(t) * \psi(2^i(t - n2^{-i})). \end{aligned} \tag{126}$$

Each term inside the last summation in Eq. (126) has its own wavelet expansion given by

$$x(t) * \psi(2^i(t - n2^{-i})) = \sum_{j,m \in Z \times Z} d_{j,m}^{i,n} \psi(2^j(t - m2^{-j})). \tag{127}$$

By substituting Eq. (127) into Eq. (126), and with rearrangement of the summations we find that

$$x(t) * g(t) = \sum_{j,m \in Z \times Z} \left[\sum_{i,n \in Z \times Z} d_{j,m}^{i,n}\ g_{i,n} \right] \psi(2^j(t - m2^{-j})). \tag{128}$$

Comparing Eq. (128) with the second line of Eq. (125) shows that

$$\begin{aligned} y_{j,m} &= \sum_{i,n \in Z \times Z} d_{j,m}^{i,n}\ g_{i,n}, \\ &= \sum_{i=-\infty}^{\infty} (\ldots, d_{j,m}^{i,-1}, d_{j,m}^{i,0}, d_{j,m}^{i,1}, \ldots) \begin{pmatrix} \vdots \\ g_{i,-1} \\ g_{i,0} \\ g_{i,1} \\ \vdots \end{pmatrix}. \end{aligned} \tag{129}$$

This suggests the following expression:

$$\boldsymbol{Y} = \mathcal{D}\ \boldsymbol{G}, \tag{130}$$

where $\mathcal{D}$ is a tensor, and $\boldsymbol{Y}$ and $\boldsymbol{G}$ are matrices. Assuming a suitably defined inverse of $\mathcal{D}$ exists, the wavelet coefficients for the expansion of $g(t)$ can be found from the expression

$$\boldsymbol{G} = \mathcal{D}^{-1}\ \boldsymbol{Y}. \tag{131}$$

A time series for the impulse response $g(t)$ can be found immediately by using coefficients $g_{i,n}$ in Eq. (77).

At this point, some comments are in order. First, the matrices and tensors in Eq. (130) contain an infinite number of elements. However, in practice one should find that elements will approach zero as the magnitude of their indices i, j, m and n become large. This follows from Theorem 2, which says the wavelet transform decays as the magnitude of s and τ become large. Since the coefficients of the wavelet expansion are

equal to the wavelet transform at each point where $(s,\tau) = (2^j, 2^{-j}k)$, we know that the coefficients will decay to zero as the magnitude of j and k become large. Thus, for practical purposes, we need only use matrices and tensors with finite numbers of significant coefficients.

Given that we will truncate the tensors and matrices defined above, the problem can be recast as a standard linear programming problem using matrices and vectors. First, from Theorem 2 we know that the coefficients for the wavelet expansion of the input $x(t)$ will only be significant for limited ranges of i and n, i.e., $i = i_l, \ldots, i_h$, and $n = n_l, \ldots, n_h$. From Eq. (127) and the orthogonality of the wavelets in the expansion, we know that we need only consider those elements of $\mathcal{D}$ associated with these values of i and n. Similarly, the coefficients for the measured output will only be significant for a range of j and m, i.e., $j = j_l, \ldots, j_h$, and $m = m_l, \ldots, m_h$. (More generally, (n_l, n_h) and (m_l, m_h) could depend on i and j respectively. This was done in the numerical example that follows.) From Eq. (125), it is implied that we need only consider those elements of $\mathcal{D}$ that are related to the coefficients for the output associated with these values of j and m. With these facts in mind and by using Eq. (130), this implies that the problem of finding the wavelet expansion of the system impulse response (finding the coefficients $g_{i,n}$) can be well approximated by the vector equation

$$\boldsymbol{y} = \boldsymbol{D}\boldsymbol{g}, \tag{132}$$

where

$$\begin{aligned}
\boldsymbol{D} &= \begin{pmatrix}
d_{j_l,m_l}^{i_l,n_l} & \cdots & d_{j_l,m_l}^{i_l,n_h} & \cdots & d_{j_l,m_l}^{i_h,n_l} & \cdots & d_{j_l,m_l}^{i_h,n_h} \\
\vdots & & \vdots & & \vdots & & \vdots \\
d_{j_l,m_h}^{i_l,n_l} & \cdots & d_{j_l,m_h}^{i_l,n_h} & \cdots & d_{j_l,m_h}^{i_h,n_l} & \cdots & d_{j_l,m_h}^{i_h,n_h} \\
\vdots & & \vdots & & \vdots & & \vdots \\
d_{j_h,m_l}^{i_l,n_l} & \cdots & d_{j_h,m_l}^{i_l,n_h} & \cdots & d_{j_h,m_l}^{i_h,n_l} & \cdots & d_{j_h,m_l}^{i_h,n_h} \\
\vdots & & \vdots & & \vdots & & \vdots \\
d_{j_h,m_h}^{i_l,n_l} & \cdots & d_{j_h,m_h}^{i_l,n_h} & \cdots & d_{j_h,m_h}^{i_h,n_l} & \cdots & d_{j_h,m_h}^{i_h,n_h}
\end{pmatrix}, \\
\boldsymbol{y}^T &= \begin{pmatrix} y_{j_l,m_l} & \cdots & y_{j_l,m_h} & \cdots & y_{j_h,m_l} & \cdots & y_{j_h,m_h} \end{pmatrix}, \\
\boldsymbol{g}^T &= \begin{pmatrix} g_{i_l,n_l} & \cdots & g_{i_l,n_h} & \cdots & g_{i_h,n_l} & \cdots & g_{i_h,n_h} \end{pmatrix}.
\end{aligned} \tag{133}$$

We see that $\mathcal{D}$ is a matrix of size $(j_h - j_l + 1)(m_h - m_l + 1) \times (i_h - i_l + 1)(n_h - n_l + 1)$, and the vectors $\boldsymbol{y}$ and $\boldsymbol{g}$ are of length $(j_h - j_l + 1)(m_h - m_l + 1)$ and $(i_h - i_l + 1)(n_h - n_l + 1)$ respectively.

If $N = (j_h - j_l + 1)(m_h - m_l + 1) = (i_h - i_l + 1)(n_h - n_l + 1)$, then $\boldsymbol{D}$ is a square matrix, and the vectors are now elements of the Euclidean space R^N. We also see that the solution $\boldsymbol{g}$ does not change if we multiply both sides by the Hermitian of $\boldsymbol{D}$, since

$$\boldsymbol{b} \doteq \boldsymbol{D}^H\boldsymbol{y} = \boldsymbol{D}^H\boldsymbol{D}\boldsymbol{g} \doteq \boldsymbol{Q}\boldsymbol{g}. \tag{134}$$

We now seek the solution to the equation

$$\boldsymbol{b} = \boldsymbol{Q}\boldsymbol{g}, \tag{135}$$

where $\boldsymbol{Q} = \boldsymbol{D}^H\boldsymbol{D}$ is now a positive definite matrix. It is now possible to show that finding the solution to Eq. (135) is equivalent to finding the solution of the quadratic problem

$$\min_{\boldsymbol{g}\in R^N}\left[\frac{1}{2}\boldsymbol{g}^H\boldsymbol{Q}\boldsymbol{g} - \boldsymbol{b}^H\boldsymbol{g}\right]. \tag{136}$$

Finding g is now recast as a minimization problem, thus allowing the use of any method designed to solve this class of problem.

We could find $\boldsymbol{g}$ by multiplying $\boldsymbol{b}$ by the inverse of $\boldsymbol{Q}$, providing $\boldsymbol{Q}$ is nonsingular. If it is, then $\boldsymbol{Q}^{-1}$ is unique, and we have a unique solution for $\boldsymbol{g}$. However, rather than finding $\boldsymbol{Q}^{-1}$ directly, we really need only to find $\boldsymbol{g}$ directly. Such a method is a numerical procedure called the *conjugate gradient algorithm* [10]. It possess the same numerical stability as the steepest decent algorithm but converges in a finite number of steps at the cost of some additional computation. This method produces a finite sequence of vectors $\boldsymbol{g}_0, \boldsymbol{g}_1, \ldots, \boldsymbol{g}_N$, where $\boldsymbol{g}_N$ is the solution we seek. The complete algorithm is given as follows. Let $\boldsymbol{g}_0$ be any vector in R^N, and define $\boldsymbol{d}_0 = -\boldsymbol{e}_0 = \boldsymbol{b} - \boldsymbol{Q}\boldsymbol{g}_0$, then for $k = 0, \ldots, (N-1)$,

$$\begin{aligned}
\boldsymbol{g}_{k+1} &= \boldsymbol{g}_k + \alpha_k\boldsymbol{d}_k, \\
\alpha_k &= -\frac{\boldsymbol{e}_k^T\boldsymbol{d}_k}{\boldsymbol{d}_k^H\boldsymbol{Q}\boldsymbol{d}_k}, \\
\boldsymbol{d}_{k+1} &= -\boldsymbol{e}_{k+1} + \beta_k\boldsymbol{d}_k, \\
\beta_k &= \frac{\boldsymbol{e}_{k+1}^H\boldsymbol{Q}\boldsymbol{d}_k}{\boldsymbol{d}_k^H\boldsymbol{Q}\boldsymbol{d}_k}, \\
\boldsymbol{e}_k &= \boldsymbol{Q}\boldsymbol{g}_k - \boldsymbol{b}.
\end{aligned} \tag{137}$$

In practice, we generally cannot measure $y(t)$ exactly but are given $y_m(t) = y(t) + n(t)$ where $n(t)$ is a noise process. This, in turn, means that we do not know $\boldsymbol{y}$ but are given $\boldsymbol{y}_m = \boldsymbol{y} + \boldsymbol{n}$, where $\boldsymbol{n}$ is the vector describing the deviation from the true value of $\boldsymbol{y}$ because of $n(t)$. Therefore, application of the conjugate gradient algorithm gives us $\boldsymbol{g}$ in a best least square error sense. As we will see, the presence of noise in $\boldsymbol{y}_m$ will cause distortion and noise to appear in the solution for $\boldsymbol{g}$ and in the resulting reconstructed time series derived from the wavelet expansion.

Figures 16 through 18 show the input $x(t)$, the noiseless output $y(t)$, and impulse response $g(t)$, the function we seek to estimate. Figures 19 through 21 show their respective wavelet transforms that were generated by using the Daubechies wavelet of order $n = 5$. Furthermore, all wavelet coefficients utilized in the deconvolution algorithm were also based on wavelet expansions using the Daubechies wavelet of order $n = 5$. Since the vector expression in Eq. (132) is an approximation to the matrix expression in Eq. (130), it is appropriate that the matrix $\boldsymbol{D}$ and vector $\boldsymbol{y}$ (or $\boldsymbol{y}_m$) are composed of the significant elements (those of largest magnitude) of the tensor $\mathcal{D}$ and matrix $\boldsymbol{Y}$ respectively. This is done by choosing carefully the ranges of i, j, n, and m.

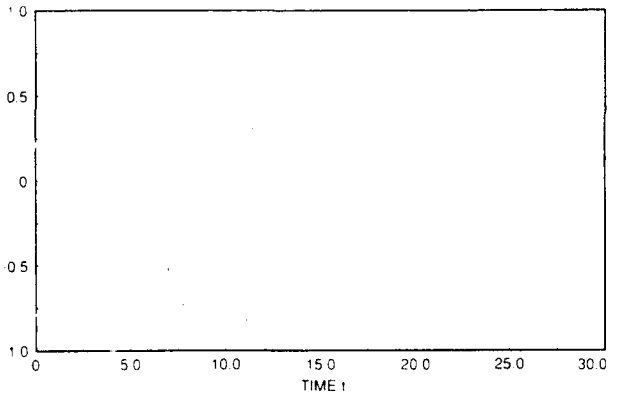

Fig. 16 — Input signal

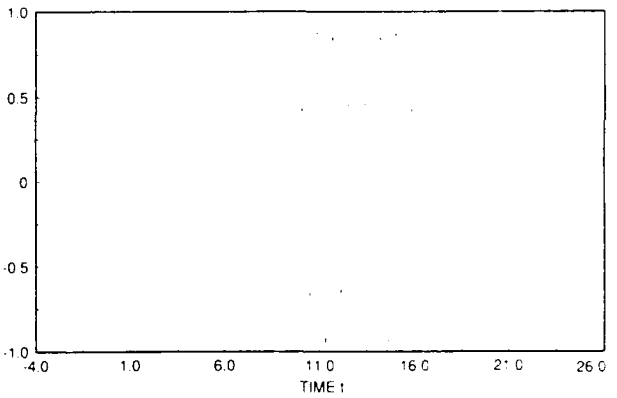

Fig. 17 — Noiseless output signal

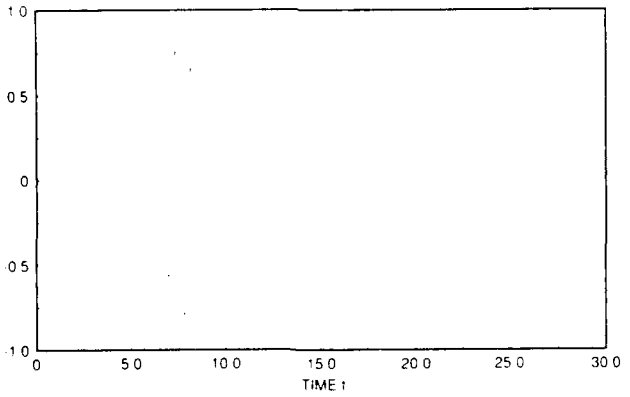

Fig. 18 — True impulse response. This is the function we seek via a deconvolution algorithm.

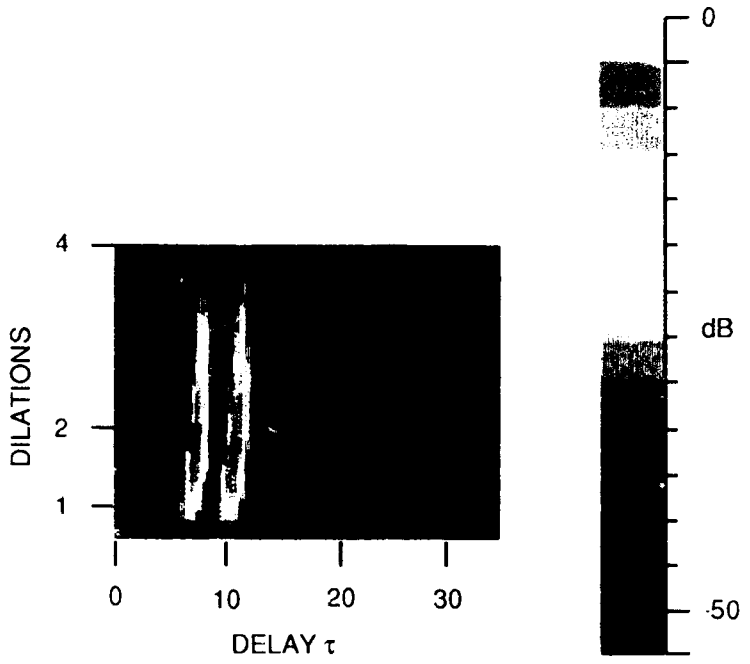

Fig. 19 – Square magnitude of the wavelet transform of the input signal. The transform kernel is a Daubechies orthogonal wavelet of order $n = 5$.

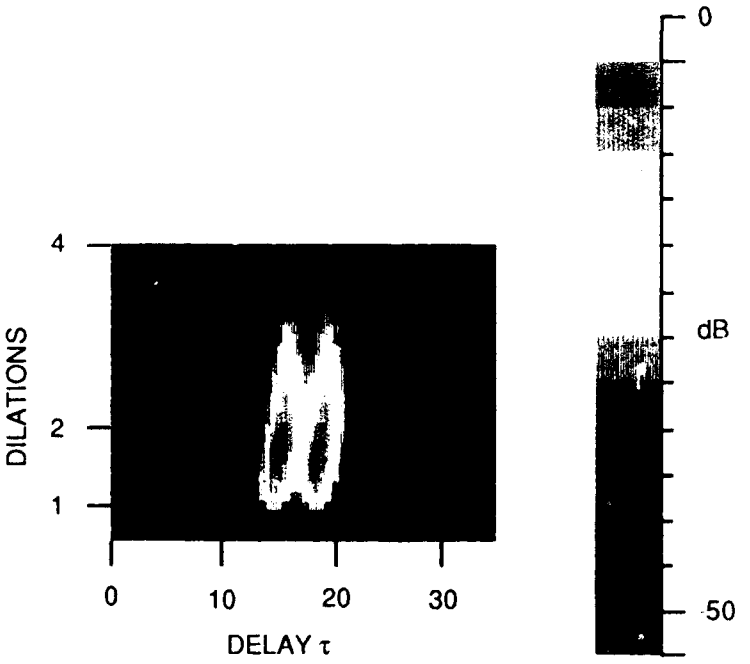

Fig. 20 – Square magnitude of the wavelet transform of the noiseless output signal. The transform kernel is a Daubechies orthogonal wavelet of order $n = 5$.

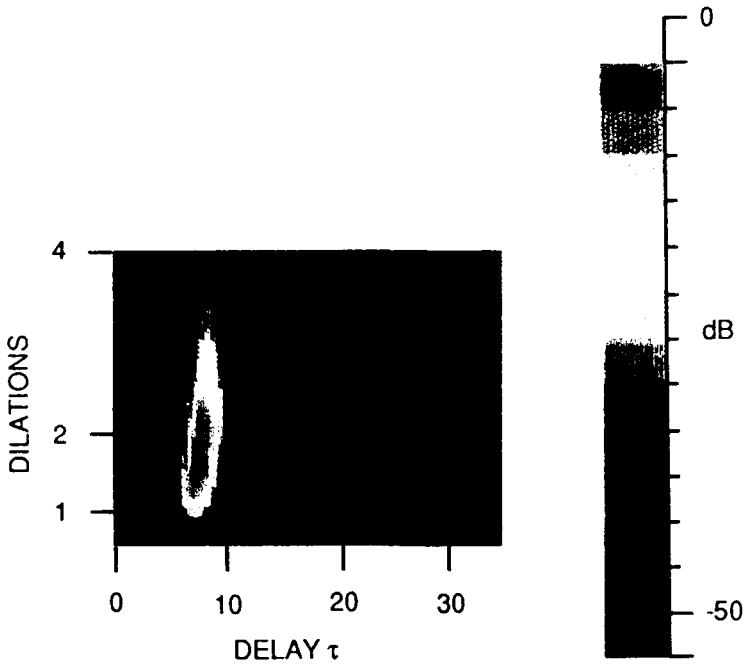

Fig. 21 — Square magnitude of the wavelet transform of the true impulse response. The transform kernel is a Daubechies orthogonal wavelet of order $n = 5$.

To choose the ranges of i and n, we consider the vector $\boldsymbol{y}_m$ (or $\boldsymbol{y}_m$) whose elements are the wavelet expansion coefficients of the (measured) output. These coefficients, in turn, are equal to the values of the wavelet transform of the (measured) output at $(s,\tau) = (2^j, 2^{-j}m)$, for $j,m \in Z \times Z$. Therefore, we choose j_l, j_h, m_l, and m_h so that $\boldsymbol{y}$ is composed of all coefficients within and on the boundary of the region $s \in [2^{-2}, 2^1]$ and $\tau \in [12, 26]$, including the coefficient $y_{-2,2}$, which is equal to the wavelet transform at $(s,\tau) = (2^{-2}, 8)$. As can be seen from Fig. 20, this region defines the portion of the (s,τ) plane where the wavelet transform of the output is significant.

We are now left with the task of choosing the ranges of i and n, and this is done by examining the elements $d^{i,n}_{j,m}$ of the matrix $\boldsymbol{D}$. If we consider Eq. (127), we can assume that the wavelet expansion coefficients of any $x * \phi(\cdot)$ should at most be significant over the ranges of i and n for which the wavelet expansion coefficients of the input $x(t)$ are significant. These coefficients, in turn, are equal to the values of the wavelet transform of the input at $(s,\tau) = (2^i, 2^{-i}n)$, for $i,n \in Z \times Z$. Therefore, we choose i_l, i_h, n_l, and n_h such that $\boldsymbol{D}$ is composed of all coefficients within and on the boundary of the region $s \in [2^{-2}, 2^1]$ and $\tau \in [2, 16]$, including the coefficient $d^{i,n}_{-2,0}$ that is equal to the wavelet transform at $(s,\tau) = (2^{-2}, 0)$. As can be seen from Fig. 19, this region defines the portion of the (s,τ) plane where the wavelet transform of the input is significant.

The choice of the ranges of i, j, n, and m for the example presented here resulted in a matrix $\boldsymbol{D}$ of size 57×57. Consequently, the conjugate gradient algorithm converged in 57 iterations. The choice of $\boldsymbol{g}_0$ (the initial guess of $\boldsymbol{g}$) is arbitrary; hence, it was set equal to a vector of zeros.

Figures 22 to 29 show the outputs with various signal-to-noise ratios and the resulting estimated impulse responses. In all cases the estimated impulse response was derived from a wavelet reconstruction using dilations 2^{-2}, 2^{-1}, 2^{0}, and 2^{1}. Clearly, as the signal-to-noise ratio of the measured output decreases the estimated impulse response becomes progressively more noisy and distorted. This also shows that high signal-to-noise ratios are required for accurate estimation of the impulse response. Such behavior is common to all deconvolution algorithms; it demonstrates a typical trade-off. Generally, convolution smears the impulse response to produce the output signal. Deconvolution buys back the resolution or features of the impulse response but at the expense of producing an estimate exhibiting a signal-to-noise ratio that is lower than the measured output [11].

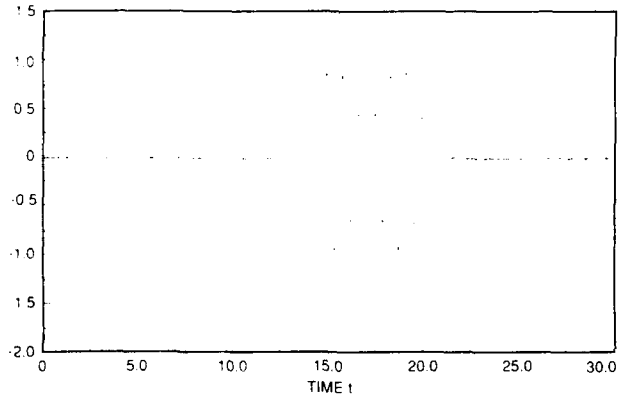

Fig. 22 — Noisy output signal with a peak-signal-to-average-noise ratio of 40 dB

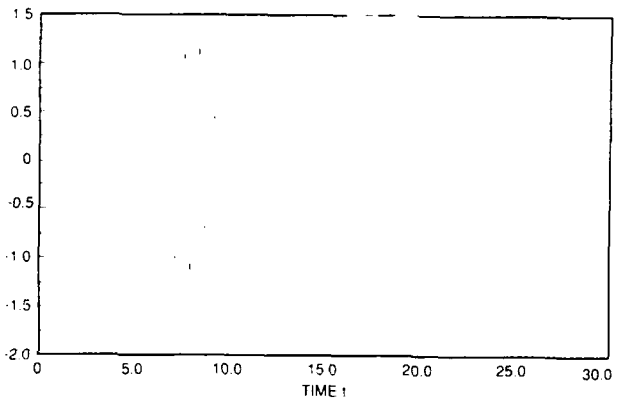

Fig. 23 — Estimated impulse response based on the input signal shown in Fig. 22 possessing a peak-signal-to-average-noise ratio of 40 dB. The wavelet expansion for the reconstruction of the impulse response used a Daubechies orthogonal wavelet of order $n = 5$, and dilations 2^{-2}, 2^{-1}, 2^{0}, and 2^{1}.

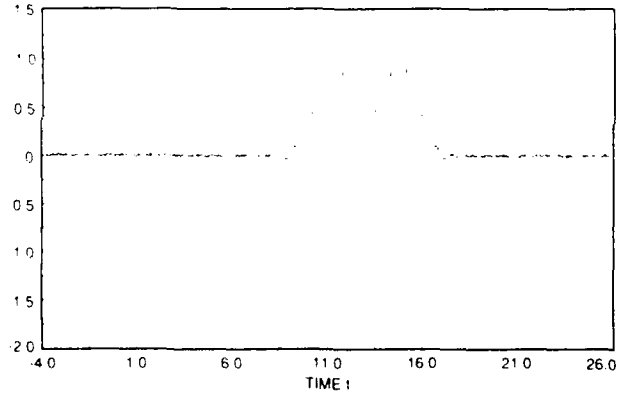

Fig. 24 — Noisy output signal with a peak-signal-to-average-noise ratio of 35 dB

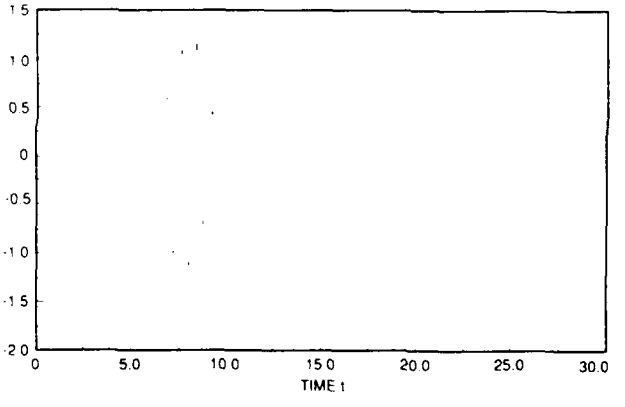

Fig. 25 — Estimated impulse response based on the input signal shown in Fig. 24 that possesses a peak-signal-to-average-noise ratio of 35 dB. The wavelet expansion for the reconstruction of the impulse response used a Daubechies orthogonal wavelet of order $n = 5$, and dilations 2^{-2}, 2^{-1}, 2^{0}, and 2^{1}.

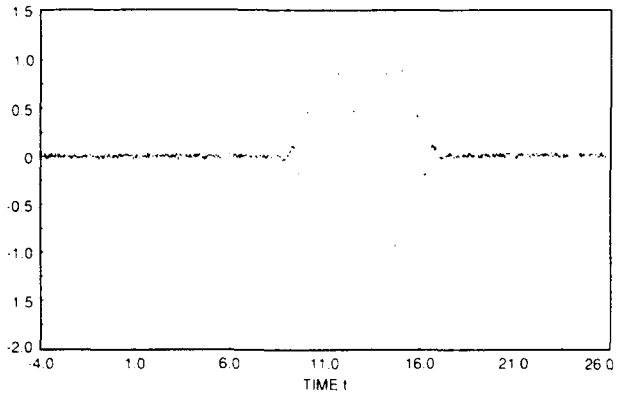

Fig. 26 — Noisy output signal with a peak-signal-to-average-noise ratio of 30 dB

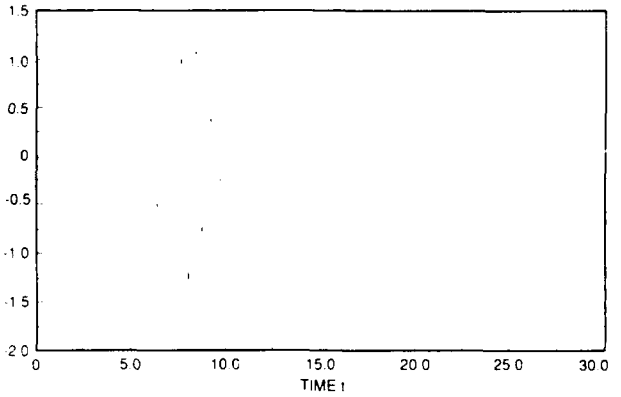

Fig. 27 — Estimated impulse response based on the input signal shown in Fig. 26 that possesses a peak-signal-to-average-noise ratio of 30 dB. The wavelet expansion for the reconstruction of the impulse response used a Daubechies orthogonal wavelet of order $n = 5$, and dilations 2^{-2}, 2^{-1}, 2^{0}, and 2^{1}.

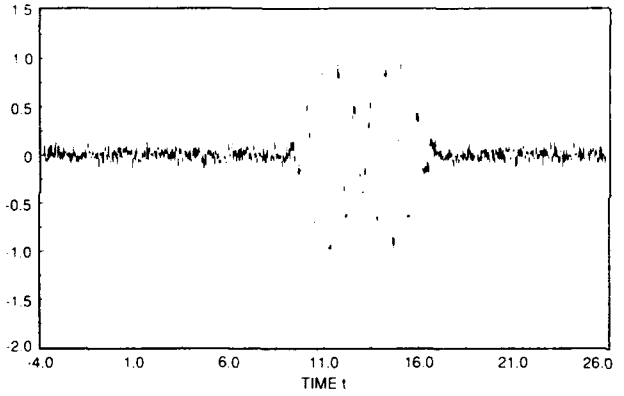

Fig. 28 — Noisy output signal with a peak-signal-to-average-noise ratio of 20 dB

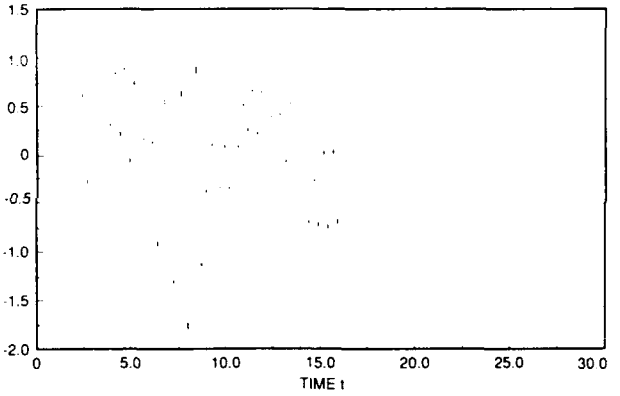

Fig. 29 — Estimated impulse response based on the input signal shown in Fig. 28 possessing a peal-signal-to-average-noise ratio of 20 dB. The wavelet expansion for the reconstruction of the impulse response used a Daubechies orthogonal wavelet of order $n = 5$, and dilations 2^{-2}, 2^{-1}, 2^{0}, and 2^{1}.

9. SUMMARY

This report addressed several theoretical and practical aspects of the wavelet transform and wavelet expansion in the context of signal theory and signal processing.

On the most general level, several theorems were proved. In particular, a 'decay rate theorem' was proved (Theorem 2) which described how rapidly the wavelet transform decays as the dilation variable s increases. Moreover, the theorem showed the decay rate depends upon the continuity of the transformed signal. Such a theorem is analogous to the various decay rate theorems found in Fourier analysis that describe how rapidly a Fourier spectrum decays as the magnitude of the frequency variable increases.

We also presented the reformulation and extension of some existing results. The material in Section 4 showed that linear system theory, i.e., input/output relationships for linear systems could be reformulated in the context of the wavelet transform. It was also shown that stochastic signal theory could be applied to the wavelet transform; the power spectral density and autocorrelation function could be used to describe the expected value of wavelet transform of a stochastic signal. Some of the material in Sections 6 and 7 extended some earlier work. Here, the continuity, boundedness, and regularity of the Daubechies orthonormal wavelets were guaranteed. Such results were only sketched out in the original presentation of her work [2].

Two practical applications of the wavelet expansion were presented. The first application was a filtering method, which may be most useful when the coefficients of the wavelet expansion are already available. Here, we showed that one could passband filter in the wavelet domain. Because of the sense of locality offered by the wavelet expansion (and wavelet transform), this filtering method may be applicable when we require short term, localized filtering of a signal. The second application of the wavelet expansion was the development of a deconvolution or iterative restoration algorithm. The method cast the problem as a quadratic least squares problem, thus admitting to a solution by a host of well known and established algorithms. In this case we chose the conjugate gradient algorithm, because it converges in a finite number of iterations. This also allowed us to avoid the problem of division by zero that crops up in the simple spectral division approach to deconvolution. The disadvantage of using the wavelet expansion approach to deconvolution is the need to precalculate the expansion coefficients, and, to date, no known analog to the fast Fourier transform (FFT) exists for the wavelet expansion. Thus, we have encountered a classic trade off: the development of a robust deconvolution algorithm at the expense of additional numerical computation.

10. REFERENCES

1. J.M.Combes, A.Grossman, P.Tchamitchian, eds., Wavelets: Time-Frequency Methods and Phase Space, Proc. of the Int. Conf., Marseille, France, Dec. 14-18, 1987 (Springer-Verlag, Berlin, Germany, 1989).

2. I.Daubechies, "Orthogonal Bases of Compactly Supported Wavelets," *Commun. on Pure and Applied Mathematics* **XLI**, 909-996 (1988).

3. I.Daubechies, "Painless nonorthogonal expansions," *J. Mathematical Physics* **27**(5), 1271-1283 (1986).

4. A.Grossmann, J.Morlet, "Decomposition of Hardy Functions into Square Integrable Wavelets of Constant Shape," *SIAM J. Mathematical Analysis* **15**(4), 723-736 (1984).

5. S.G.Mallat, "A Theory for Multiresolution Signal Decomposition: The Wavelet Representation," *IEEE Trans. Pattern Analysis and Machine Intelligence* **11**(7), 674-693 (1989).

6. A.Papoulis, *Probability, Random Variables, and Stochastic Processes*, 2nd ed. (McGraw-Hill, New York, NY, 1984).

7. R.S.Kennedy, *Fading Dispersive Channels* (John Wiley and Sons, New York, NY, 1969).

8. L.J.Ziomek, *Underwater Acoustics: A Linear System Theory Approach*, (Academic Press, New York, NY, 1985).

9. D.E.Johnson, *Introduction to Filter Theory* (Prentice-Hall, Englewood Cliffs, NJ, 1976).

10. D.G.Luenberger, *Linear and Nonlinear Programming, 2nd ed.* (Addison-Wesley Publishing Co., Reading MA, 1984).

11. R.W.Schafer, R.M.Mersereau, M.A.Richards, "Constrained Iterative Restoration Algorithms," *Proc. IEEE* **69**(4), 432-450 (1981).

Appendix A

FOURIER SERIES COEFFICIENTS FOR DAUBECHIES WAVELETS

Note that the coefficients listed below define the Fourier series

$$H_n(f) = 2^{-1/2} \sum_{k=0}^{2n-1} a_n(k) e^{-j2\pi kf}, \qquad (A1)$$

which is consistent with Daubechies definition of the series $H_n(f)$ [2]. To be consistent with the form of $H_n(f)$ used in Eq. (82), one must take $h_n(k) = a_n(k)/\sqrt{2}$.

$$\begin{aligned} a_2(0) &= 0.482962913145 \\ a_2(1) &= 0.836516303738 \\ a_2(2) &= 0.224143868042 \\ a_2(3) &= -.129409522551 \end{aligned}$$

$$\begin{aligned} a_3(0) &= 0.332670552950 \\ a_3(1) &= 0.806891509311 \\ a_3(2) &= 0.459877502118 \\ a_3(3) &= -.135011020010 \\ a_3(4) &= -.085441273882 \\ a_3(5) &= 0.035226291882 \end{aligned}$$

$$\begin{aligned} a_4(0) &= 0.230377813309 \\ a_4(1) &= 0.714846570553 \\ a_4(2) &= 0.630880767930 \\ a_4(3) &= -.027983769417 \\ a_4(4) &= -.187034811719 \\ a_4(5) &= 0.030841381836 \\ a_4(6) &= 0.032883011667 \\ a_4(7) &= -.010597401785 \end{aligned}$$

$$\begin{aligned} a_5(0) &= 0.160102397974 \\ a_5(1) &= 0.603829269797 \\ a_5(2) &= 0.724308528438 \\ a_5(3) &= 0.138428145901 \\ a_5(4) &= -.242294887066 \\ a_5(5) &= -.032244869585 \\ a_5(6) &= 0.077571493840 \\ a_5(7) &= -.006241490213 \\ a_5(8) &= -.012580751999 \\ a_5(9) &= 0.003335725285 \end{aligned}$$

$$
\begin{aligned}
a_6(0) &= 0.111540743350 & a_6(6) &= 0.097501605587 \\
a_6(1) &= 0.494623890398 & a_5(7) &= 0.027522865530 \\
a_6(2) &= 0.751133908021 & a_6(8) &= -.031582039318 \\
a_6(3) &= 0.315250351709 & a_6(9) &= 0.000553842201 \\
a_6(4) &= -.226264693965 & a_6(10) &= 0.004777257511 \\
a_6(5) &= -.129766867567 & a_6(11) &= -.001077301085
\end{aligned}
$$

$$
\begin{aligned}
a_7(0) &= 0.077852054085 & a_7(7) &= 0.080612609151 \\
a_7(1) &= 0.396539319482 & a_7(8) &= -.038029936935 \\
a_7(2) &= 0.729132090846 & a_7(9) &= -.016574541631 \\
a_7(3) &= 0.469782287405 & a_7(10) &= 0.012550998556 \\
a_7(4) &= -.143906003929 & a_7(11) &= 0.000429577973 \\
a_7(5) &= -.224036184994 & a_7(12) &= -.001801640704 \\
a_7(6) &= 0.071309219267 & a_7(13) &= 0.000353713800
\end{aligned}
$$

$$
\begin{aligned}
a_8(0) &= 0.054415842243 & a_8(8) &= -.017369301002 \\
a_8(1) &= 0.312871590914 & a_8(9) &= -.044088253931 \\
a_8(2) &= 0.675630736297 & a_8(10) &= 0.013981027917 \\
a_8(3) &= 0.585354683654 & a_8(11) &= 0.008746094047 \\
a_8(4) &= -.015829105256 & a_8(12) &= -.004870352993 \\
a_8(5) &= -.284015542962 & a_8(13) &= -.000391740373 \\
a_8(6) &= 0.000472484574 & a_8(14) &= 0.000675449406 \\
a_8(7) &= 0.128747426620 & a_8(15) &= -.000117476784
\end{aligned}
$$

$$
\begin{aligned}
a_9(0) &= 0.038077947364 & a_9(9) &= -.067632829061\\
a_9(1) &= 0.243834674613 & a_9(10) &= 0.000250947115\\
a_9(2) &= 0.604823123690 & a_9(11) &= 0.022361662124\\
a_9(3) &= 0.657288078051 & a_9(12) &= -.004723204758\\
a_9(4) &= 0.133197385825 & a_9(13) &= -.004281503682\\
a_9(5) &= -.293273783279 & a_9(14) &= 0.001847646883\\
a_9(6) &= -.096840783223 & a_9(15) &= 0.000230385764\\
a_9(7) &= 0.148540749338 & a_9(16) &= -.000251963189\\
a_9(8) &= 0.030725681479 & a_9(17) &= 0.000039347320
\end{aligned}
$$

$$
\begin{aligned}
a_{10}(0) &= 0.026670057901 & a_{10}(10) &= -.029457536822\\
a_{10}(1) &= 0.188176800078 & a_{10}(11) &= 0.033212674059\\
a_{10}(2) &= 0.527201188932 & a_{10}(12) &= 0.003606553567\\
a_{10}(3) &= 0.688459039454 & a_{10}(13) &= -.010733175483\\
a_{10}(4) &= 0.281172343661 & a_{10}(14) &= 0.001395351747\\
a_{10}(5) &= -.249846424327 & a_{10}(15) &= 0.001992405295\\
a_{10}(6) &= -.195946274377 & a_{10}(16) &= -.000685856695\\
a_{10}(7) &= 0.127369340336 & a_{10}(17) &= -.000116466855\\
a_{10}(8) &= 0.093057364604 & a_{10}(18) &= 0.000093588670\\
a_{10}(9) &= -.071394147166 & a_{10}(19) &= -.000013264203
\end{aligned}
$$

$$
\begin{aligned}
a_{11}(0) &= 0.018692339500 & a_{11}(11) &= 0.031336714900\\
a_{11}(1) &= 0.144048360129 & a_{11}(12) &= 0.020839548328\\
a_{11}(2) &= 0.449822419238 & a_{11}(13) &= -.015365977170\\
a_{11}(3) &= 0.685506451221 & a_{11}(14) &= -.003339972936\\
a_{11}(4) &= 0.411710892303 & a_{11}(15) &= 0.004928945867\\
a_{11}(5) &= -.162485521339 & a_{11}(16) &= -.000308709907\\
a_{11}(6) &= -.274320974144 & a_{11}(17) &= -.000893056839\\
a_{11}(7) &= 0.066025638763 & a_{11}(18) &= 0.000249184997\\
a_{11}(8) &= 0.149791844607 & a_{11}(19) &= 0.000054438816\\
a_{11}(9) &= -.046504355457 & a_{11}(20) &= -.000034637754\\
a_{11}(10) &= -.066445800596 & a_{11}(21) &= 0.000004494745
\end{aligned}
$$

$$
\begin{aligned}
a_{12}(0) &= 0.013114280902 & a_{12}(12) &= 0.041627451082 \\
a_{12}(1) &= 0.109587064387 & a_{12}(13) &= -.012180151045 \\
a_{12}(2) &= 0.377449392844 & a_{12}(14) &= -.012829445168 \\
a_{12}(3) &= 0.657445006413 & a_{12}(15) &= 0.006713258423 \\
a_{12}(4) &= 0.516294170295 & a_{12}(16) &= 0.002249393038 \\
a_{12}(5) &= -.044313624533 & a_{12}(17) &= -.002179176553 \\
a_{12}(6) &= -.315809615475 & a_{12}(18) &= 0.000006459278 \\
a_{12}(7) &= -.023471399498 & a_{12}(19) &= 0.000388621871 \\
a_{12}(8) &= 0.182806918672 & a_{12}(20) &= -.000088486615 \\
a_{12}(9) &= 0.005686977952 & a_{12}(21) &= -.000024241195 \\
a_{12}(10) &= -.096186633657 & a_{12}(22) &= 0.000012775434 \\
a_{12}(11) &= 0.010995853244 & a_{12}(23) &= -.000001528836
\end{aligned}
$$

$$
\begin{aligned}
a_{13}(0) &= 0.009204916897 & a_{13}(13) &= 0.002363616024 \\
a_{13}(1) &= 0.082889405900 & a_{13}(14) &= -.023833745174 \\
a_{13}(2) &= 0.312115898739 & a_{13}(15) &= 0.003917927648 \\
a_{13}(3) &= 0.611313131287 & a_{13}(16) &= 0.007254616037 \\
a_{13}(4) &= 0.589096065406 & a_{13}(17) &= -.002760408506 \\
a_{13}(5) &= 0.086639694877 & a_{13}(18) &= -.001315670455 \\
a_{13}(6) &= -.316237370186 & a_{13}(19) &= 0.000932006061 \\
a_{13}(7) &= -.126430468961 & a_{13}(20) &= 0.000049301053 \\
a_{13}(8) &= 0.177816118862 & a_{13}(21) &= -.000165090932 \\
a_{13}(9) &= 0.071915527849 & a_{13}(22) &= 0.000030664729 \\
a_{13}(10) &= -.106342427892 & a_{13}(23) &= 0.000010440501 \\
a_{13}(11) &= -.026758244166 & a_{13}(24) &= -.000004699171 \\
a_{13}(12) &= 0.056034390582 & a_{13}(25) &= 0.000000521846
\end{aligned}
$$

$$
\begin{aligned}
a_{14}(0) &= 0.006547491642 & a_{14}(14) &= -.029754599557 \\
a_{14}(1) &= 0.063360170581 & a_{14}(15) &= -.005754062318 \\
a_{14}(2) &= 0.259953209778 & a_{14}(16) &= 0.012711190182 \\
a_{14}(3) &= 0.569486757657 & a_{14}(17) &= -.000664409841 \\
a_{14}(4) &= 0.659765991407 & a_{14}(18) &= -.003831834380 \\
a_{14}(5) &= 0.253248224211 & a_{14}(19) &= 0.001038385046 \\
a_{14}(6) &= -.245883485949 & a_{14}(20) &= 0.000708200880 \\
a_{14}(7) &= -.207221475070 & a_{14}(21) &= -.000381870689 \\
a_{14}(8) &= 0.141972692112 & a_{14}(22) &= -.000042656957 \\
a_{14}(9) &= 0.144030955893 & a_{14}(23) &= 0.000068164760 \\
a_{14}(10) &= -.083519992219 & a_{14}(24) &= -.000010124883 \\
a_{14}(11) &= -.071278880702 & a_{14}(25) &= -.000004370468 \\
a_{14}(12) &= 0.054864716315 & a_{14}(26) &= 0.000001706613 \\
a_{14}(13) &= 0.027555092282 & a_{14}(27) &= -.000000176357
\end{aligned}
$$